

UNITED STATES DEPARTMENT OF COMMERCE  
Maurice H. Stans, Secretary  
NATIONAL BUREAU OF STANDARDS ● Lewis M. Branscomb, Director



## TECHNICAL NOTE 382

ISSUED OCTOBER 1969

Nat. Bur. Stand. (U.S.), Tech. Note 382, 64 pages (Oct. 1969)

### **Laser Power and Energy Measurements**

D. A. Jennings, E. D. West, K. M. Evenson  
A. L. Rasmussen, and W. R. Simmons

Quantum Electronics Section  
Radio Standards Physics Division  
Institute for Basic Standards  
National Bureau of Standards  
Boulder, Colorado 80302

NBS Technical Notes are designed to supplement the Bureau's regular publications program. They provide a means for making available scientific data that are of transient or limited interest. Technical Notes may be listed or referred to in the open literature.

---

For sale by the Superintendent of Documents, U.S. Government Printing Office, Washington, D.C. 20402  
(Order by SD Catalog No. C13.46:382), Price 65 cents

## Table of Contents

	Page
List of Tables . . . . .	iv
List of Figures . . . . .	v
Abstract . . . . .	1
1. Introduction . . . . .	2
2. Theoretical Background for Laser Calorimetry . . . . .	5
2.1 An Application of the Theory . . . . .	15
3. Energy Measurements . . . . .	21
3.1 Introduction . . . . .	21
3.2 The Calorimeter . . . . .	21
3.3 Methods of Calibration . . . . .	23
a. Heat Capacity Calibration . . . . .	24
b. DC Electrical Energy Calibration . . . . .	24
c. Reflecting Plate Calibration . . . . .	25
3.4 Logarithmical Extrapolation . . . . .	25
3.5 Intercomparisons Using Liquid Cell Calorimeter . . . . .	27
3.6 Intercomparisons Using Metal Reflecting Plate Calorimeter . . . . .	31
3.7 Other Parts of the System . . . . .	36
4. CW Power Measurements . . . . .	39
4.1 General Description . . . . .	39
5. CW Power Measurements in Excess of 1 Watt . . . . .	47
5.1 Introduction . . . . .	47
5.2 Calorimeters . . . . .	47
a. Disc Power Meter . . . . .	47
b. Cone-Disc Power Meter . . . . .	50
c. The Cone-Flow Power Meter . . . . .	52
6. Data Reduction for the Liquid Cell Calorimeter . . . . .	54

List of Tables

	Page
2-1. Comparison of methods of data analysis . . . . .	10
2-2. Dependence of calibration factor on heater location . . . . .	16
5-1. Reflectivities of various materials at 10.6 microns compared with polished copper . . . . .	48
6-1. Data for Electrical Input. . . . .	59

## List of Figures

		Page
2-1.	Temperature-time curve to illustrate heat-flow problem . . .	8
2-2.	Temperature-time curve for an isoperibol calorimeter . . .	8
2-3.	Calibrating Heaters . . . . .	14
2-4.	Temperature-time curves for calibrating heaters . . . . .	18
3-1.	Cross-sectional diagram of the calorimeter. . . . .	20
3-2.	Cross-sectional diagram of the calorimeter absorption cell .	22
3-3.	Diagram for comparison of calorimeters. . . . .	28
3-4.	Diagram for comparison of calorimeters. . . . .	28
3-5.	Photo of apparatus for comparison of calorimeters . . . . .	29
3-6.	Diagram for calibration of beam splitters . . . . .	32
3-7.	Diagram for comparison for liquid cell and reflecting plate calorimeters. . . . .	34
4-1.	Schematic of the CW laser power meter calibration system .	38
4-2.	Diagram showing the basic calibration procedure. . . . .	40
4-3.	The response of the liquid cell calorimeter to a CW laser beam. . . . .	42
4-4.	Transfer detector calibration as a function of laser power. .	44
5-1.	Schematic of the copper disc calorimeter showing construction details . . . . .	46
5-2.	Schematic of the cone-disc power meter showing construction details. . . . .	49
5-3.	Schematic of the cone-flow power meter showing construction details. . . . .	51
6-1.	Response of calorimeter to a DC electrical energy pulse. . .	57
6-2.	Example of the results of using the integration procedure in determining the amount of energy in a laser pulse. . . . .	61

## Laser Power and Energy Measurements

D. A. Jennings, E. D. West, K. M. Evenson  
A. L. Rasmussen and W. R. Simmons

Most laser calorimeters operate in a constant temperature environment. The calorimeters can be used as deflection devices or the data can be analyzed by extrapolation or integration. Consideration of the heat flow problem common to all of these methods points up the underlying assumptions and the possible errors involved.

Calorimeters for measuring the output energy of pulsed ruby and neodymium glass lasers have been built and calibrated. The absorbing medium is an aqueous solution of  $\text{CuSO}_4$ . Calibration of laser energy detectors has an estimated uncertainty of  $\pm 2\%$  for input energies of 0.1J to 1.00J. Comparisons of absorption cell calorimeters with metal plate calorimeters agree within 1%.

Instrumentation is described that is used for the calibration of CW laser power meters. The calibration unit employs an absorption cell calorimeter to calibrate the output of a photovoltaic cell transfer detector. The power meter to be calibrated is then compared to the calibrated output of the transfer detector. The calibrations are within an accuracy of 4%.

A discussion and description is also given of several types of calorimeters that have been used to measure the output of a 100 watt CO<sub>2</sub> laser. The most recent design provides for measurement from 1 watt to 5 kilowatts with a measured accuracy of better than 3%.

Key words: Calorimetry; laser; laser calorimetry; laser energy; laser power.

## 1. Introduction

The field of laser power and energy measurements is a relatively new one which presents a wide variety of problems. Heard<sup>(1)</sup> and Birnbaum and Birnbaum<sup>(2)</sup> have reviewed the work in this field. Measurements are required for wavelengths from 400 nm to 30  $\mu$ m, for power levels from  $10^{-6}$  to  $10^{12}$  watts, for energies from  $10^{-3}$  to  $10^3$  joules, and for operating conditions ranging from single pulses through repetitive pulses to continuous wave.

Measuring devices which are relatively insensitive to wavelength are desirable because the greater the useful range, the fewer the devices which must be designed, tested, calibrated, and maintained. An advantage of calorimeters, which convert radiant energy to heat and measure the quantity of heat, is that they can be designed to operate over a large range of wavelengths.

The large ranges of power and energy to be measured require a considerable number of devices because the range of any one device is relatively limited. There are considerable problems of scaling and intercomparison to insure consistency of measurements at the various

levels. Large power levels present a special problem because of possible damage to the measuring device. The damage apparently results not only from thermal effects but also from the large electrical fields due to the coherence of the radiation.

The operating conditions also affect the measurement. Single pulses usually require an energy measurement. The output of CW and most repetitively pulsed lasers can be measured either continuously as power or as energy by letting the beam into the calorimeter for a known time.

With such a variety of problems in a rapidly growing field, many problems remain to be solved. However, there is an immediate practical need for measurements. We hope that this Technical Note will help with some of these immediate problems.

As remarked in the foreword, this note is a summary of lectures given at a seminar on laser power and energy measurements. The lecturers represented several different laboratories at the National Bureau of Standards, so that the various sections are, to a large extent, independent of one another. They are not intended to be read in sequence, but rather for the particular topics of interest.

The lectures contained a good deal of information on unsatisfactory methods and techniques. This information has been retained in the belief that, in the present state of the art, knowledge of some of the pitfalls to avoid can be practically useful.

Section 2 attempts to show how the behavior of calorimeters follows from and is predictable from the boundary value problem describing heat flow in the calorimeter. It might be read for possible insights into the behavior of calorimeter, but not to find out how a particular measurement is made at NBS.

Section 3 deals with energy measurements, particularly with respect to the liquid cell calorimeter and its application in testing other devices. Many of the practical considerations of laser power and energy measurements are discussed in this section.

Section 4 deals with the comparison of the liquid cell calorimeter, an energy measuring device, to power measuring devices, using a silicon cell as a transfer detector.

Section 5 discusses several devices used for measurement at CW power levels from one watt to five kilowatts.

Section 6 discusses the treatment of data primarily with respect to the liquid cell calorimeter

#### References

1. H. S. Heard, Laser Parameter Measurements Handbook, John Wiley and Sons, New York, 1968.
2. G. Birnbaum and M. Birnbaum, Proceedings IEEE 55, 1026 (1967).



## 2. Theoretical Background for Laser Calorimetry

The problems of laser power and energy measurements are relatively new--so new that some of the measurement ideas used in older fields have not yet been generally adopted. One of these ideas is that there should be a theory of the measurement. Failure to state the theory of the measurement prevents independent judgment of the validity of the measurement. If the purpose of the measurement is to convince others, the lack of a theory is an obvious handicap. Branscomb<sup>(1)</sup> has discussed this point in an article "Is the Literature Worth Retrieving?" Cameron and Plumb<sup>(2)</sup> put the theory first: "We begin with a physical theory . . ."

The measurement theory is just a statement of how one believes his apparatus works. The actual operation can then be checked against the theory and both the validity of the experimental checks and the theory itself can be judged independently. It seems obvious that one measurement may be better than another because it is based on a better theory.

Many laser power and energy measurements are made with devices which convert radiant energy to heat and measure a change in temperature. They are variously called detectors, thermopiles, bolometers, and calorimeters. Those that operate in a constant temperature environment have a common theoretical basis; i. e. they can be analyzed in terms of a common heat flow problem. Calorimeters of this type are called isoperibol calorimeters<sup>(3)</sup> and are used extensively in thermochemistry. These calorimeters can be used in a variety of ways, some of which provide a simpler and faster analysis of the data. The basic assumptions of these methods usually require experimental justification. Our purpose here is to indicate the general theoretical basis of these methods and point out the assumptions and possible errors underlying them.

The first law of thermodynamics is variously regarded as a statement of conservation of energy, as a statement of the mechanical equivalent of heat, or as just a bookkeeping procedure for accounting for energy. Regardless of philosophical views, the theory of calorimetric measurement is based on the first law: the calorimeter is a thermodynamic system, described in terms of state variables, for which the work done and heat transferred must be evaluated. A qualitative understanding of the implications of the first law--and the heat flow equations derived from it--are important to anyone either using or designing calorimeters. One should be able to answer the question, "What is the theory of the measurement?"

The laser calorimetry problem from a very practical standpoint, can be divided into three subproblems, each of which can be considered separately:

1. Materials problem--destruction by high-power.
2. Fraction of beam absorbed.
3. Measurement of the absorbed energy.

These practical problems relate in a rather direct way to the ideas in the first law, which equates the increase,  $\Delta U$ , in the internal energy of the calorimeter, to the heat,  $Q$ , transferred to the calorimeter plus the work,  $W$ , done on the calorimeter. In symbols

$$\Delta U = Q + W. \quad (1)$$

These quantities can be related to the three practical problems:

1. For the change in internal energy, we must specify the state of the system; i. e., did the beam alter the amount or chemical composition of the materials in the calorimeter?
2. We must know that the observed temperature is a measure of the internal energy, and that the temperature observation accounts for the heat exchange to the required accuracy.

3. The beam can be considered to do electromagnetic work on the calorimeter. To evaluate this work, the fraction of work converted to heat in the calorimeter and the fraction reflected back out must be known.

From an idealistic point of view, one should start with the basic theory and design a calorimeter and a method of operation. This approach can be very exacting and tedious. The theory of isoperibol calorimeters has been treated in a rather sophisticated way<sup>(4)</sup> and also with a very simple model<sup>(5)</sup> which suggests many of the same measurement techniques.

It is not practical to present a theory for all kinds of calorimetry, but a simple example shows how direct reference to the theory serves to pinpoint the assumptions which must be satisfied for a measurement to be valid.

Consider a calorimeter located in a constant temperature environment. It starts off at the same temperature as the environment and then receives a unit energy pulse from a laser at time  $t = 0$ . The output, which is the observed temperature may behave qualitatively as in figure 2-1.

The theory for this measurement follows from the heat flow problem, related to the comparison of single laser pulses. The equation for the conduction of heat is as follows:

$$\nabla \lambda (P) \nabla T(P, t) = c(P) \frac{\partial T}{\partial t} , \quad (2)$$

where the symbols have the following meanings:

$\lambda (P)$  Thermal conductivity as a function of position, but not of temperature or time.

$\nabla = \text{del} =$  the vector operator. The argument is independent of the coordinate system.

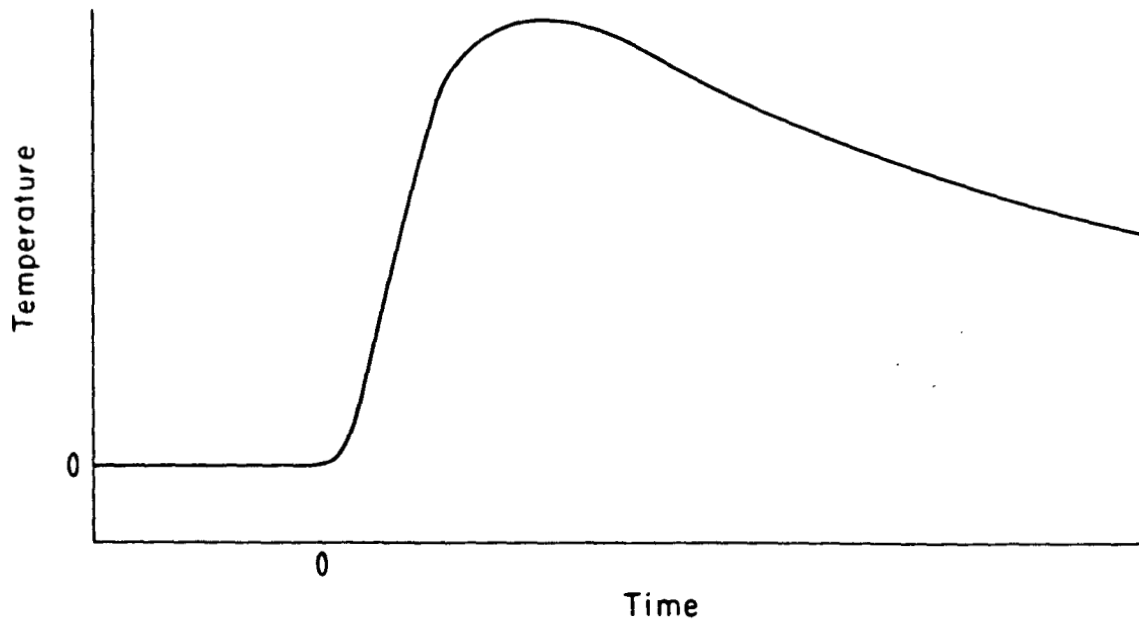


Figure 2-1. Temperature-time curve to illustrate the heat-flow problem. The calorimeter temperature is constant before the input and exponential for large values of time.

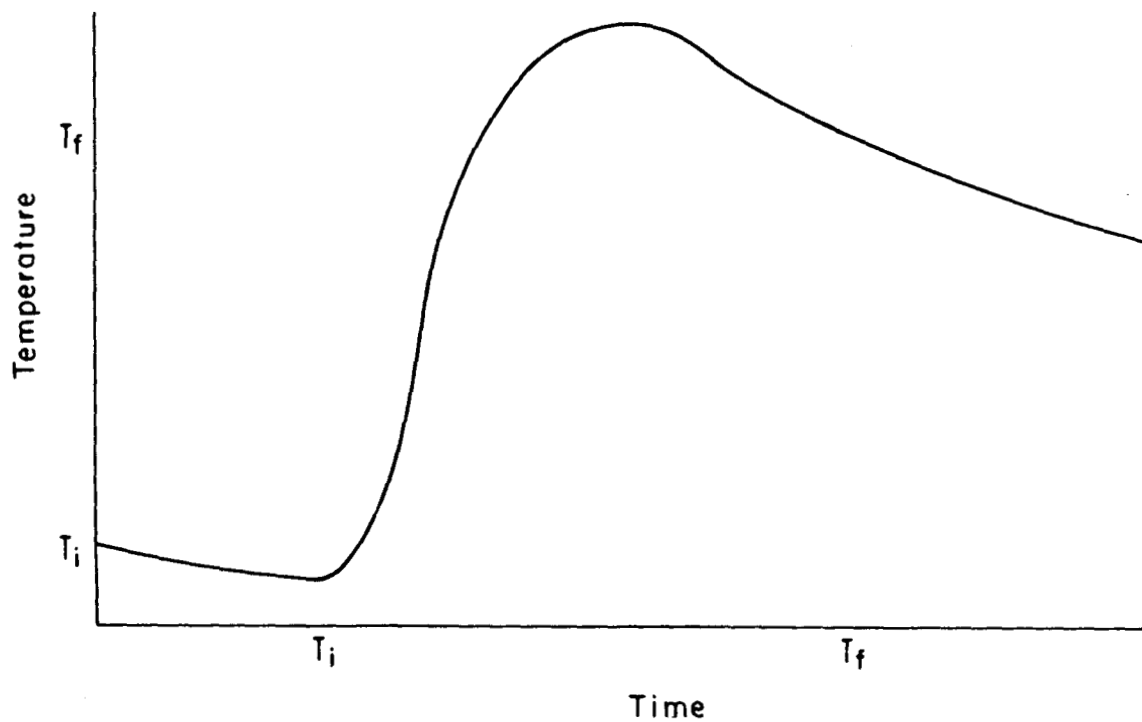


Figure 2-2. Temperature-time curve for an isoperibol calorimeter when both the initial and final temperatures are single exponential functions of time.

$T(P, t)$  Temperature as a function of position and time.

$c(P)$  Heat capacity as a function of position.

Equation (2) equates the difference in heat flowing into a volume  $dV$  in time  $dt$  to the change in the energy stored in the volume in the same time.

The boundary value of the temperature is the temperature of the surroundings, which we take as the reference temperature for this particular problem. On a boundary where there is thermal contact:

$$T = 0. \quad (3)$$

On a boundary of the calorimeter which radiates to the surroundings

$$-\lambda \frac{\partial T}{\partial n} = h T, \quad (4)$$

where  $\partial T / \partial n$  is the derivative normal to the surface and  $h$  is the coefficient for heat transfer.

Before the pulse, the entire calorimeter is at the temperature of the surroundings. The pulse at time zero sets up a temperature distribution has the geometrical distribution  $g(P)$

$$T(P, 0) = g(P). \quad (5)$$

There is a solution,  $T$ , to this boundary value problem. Now consider a pulse  $k$  times as large but having the same geometric distribution  $g(P)$ ; that is,  $T_2(P, 0) = k \cdot g(P)$ . Practically, this means having the same fraction of the energy in the same part of the beam and the beam striking the same parts of the calorimeter. Now, we say

$$T_2(P, t) = k T_1(P, t), \quad (6)$$

which is proved by substituting  $kT_1$  in the equations for  $T_2$  and obtaining

the equations for  $T_1$ . The  $k$  will factor in all cases, giving the boundary value problem which defines  $T_1$ .

To compare the two energies, eq (6) requires only that the temperature be read at equal times after the laser pulse. The time is at the discretion of the operator, but the maximum deflection is the easiest to read and gives the best precision.

This simple idea is illustrated by data for two pulses from a ruby laser. The calorimeter and laser were not moved between experiments so that the geometric energy distribution in the calorimeter would be nearly the same. The data were analyzed by this shortcut deflection method and also by the conventional calorimetric method of eq (8) carried out on a computer.

Table 2-1

	Maximum Deflection (15 sec)	Computer Analysis (12 min)
First pulse	130.2 $\mu v$	134.1 $\mu v$
Second pulse	87.7	91.4
Ratio	1.49	1.47

These ratios agree about as well as could be expected on a statistical basis.

If control of the environment is a problem, the deflection method may be more accurate. To understand why, let's go back to theory.

In the heat flow problem, the temperature of the surroundings is assumed to be constant. In the calorimeter used here this temperature may change by one or two milliKelvin during an experiment in violation of the assumption. This change may be the largest single error in the calorimeter, because the temperature is measured by a thermopile with cold junctions attached to the environment. The de-

deflection experiment may actually give a better comparison of two beams for which  $g(P)$  is the same, because the change in the temperature of the reference junction is less.

What about CW comparisons? It can be shown that comparisons are rigorous (no new approximations) where the laser power is of the form

$$P_L = k f(t) g(P). \quad (7)$$

What is meant by the same  $f(t)$ ? Comparison of two step inputs is a common case. Other examples: CW inputs or electrical heating for the same length of time. The power need not be the same.

A different problem arises when two laser beams having different relative power densities are compared or when the calorimeter is moved relative to the beam. Then the geometric distribution of the beam is changed and it is necessary to show that the small change in the geometrical distribution does not affect the result significantly. The key word here is significantly--insignificant in one application may be disastrous in another. Since the procedure violates the theory, a theoretical argument is useless. On the other hand, an experimental approach would be quite convincing. Moving the calorimeter around in a beam of constant energy, for example, would show whether the response was constant within tolerable limits. Unfortunately, it's hard to get the same response for different geometrical distribution of the absorbed energy, but people have managed to find different combinations which are adequate for their problems.

One further application of the deflection method merits consideration. Suppose that a CW laser is to be compared with a pulsed laser and suppose the difference in response due to the geometrical distribution of energy is negligible. The time dependence of the two

inputs still violates the theory; only those inputs which are the same function of time can be compared rigorously. Pulses are step energy inputs; CW are ramps. It seems fairly obvious that very short CW inputs approximate pulses. A 20 sec and a 40 sec input which give equivalent output, are evidence for an adequate comparison.

The same reasoning applies to absolute calibrations against electrical inputs. The electric heater may have both a different geometrical and a different time distribution from the laser beams to be measured. The deflection method can be justified for this case, too, on the basis of suitable experimental demonstration of behavior. Practically there are many problems with the deflection method which have caused people to seek other methods, especially when they need a little more accuracy.

Conventional calorimetry has not been widely used in laser power and energy measurements, probably because it is slow and requires considerable data reduction. For accurate work it has considerable advantages. One problem that needs particular attention is whether relatively rapid methods can be based rigorously on the more accurate but slower conventional calorimetry, perhaps the same calorimeter used by conventional and deflection methods.

The basic theory for a conventional calorimeter operating in a constant temperature surroundings is described by essentially the same boundary value problem. The development is more complicated, but the results are summarized in the equation:

$$M [ T_f - T_i + c \int_{t_i}^{t_f} (T - T_{surr}) dt ] = \Delta U_L \text{ or } \Delta U_{el} \quad (8)$$



$T$  is the observed temperature and  $E$  is the energy equivalent determined by a known electrical input. The term energy equivalent has been used to emphasize that  $E$  is not exactly a sum of heat capacities<sup>(4, 5)</sup>.

$T_{\text{surr}}$  is the temperature of the surroundings, determined by (9),  
 $t$  is the time,

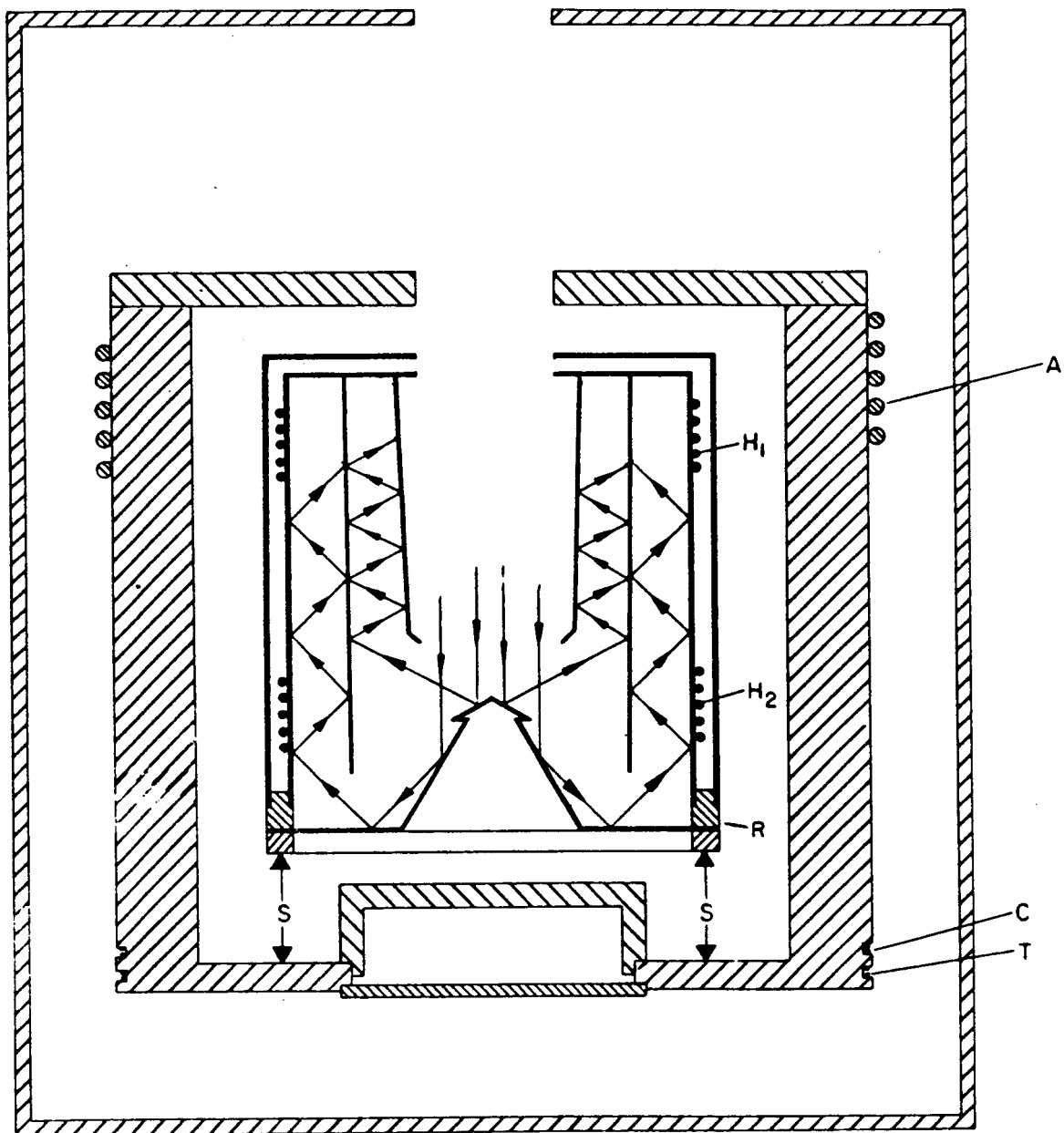
$\epsilon$  is the "cooling constant", determined from the relationship

$$dT/dt = -\epsilon (T - T_{\text{surr}}) , \quad (9)$$

$\Delta U_L$  is the energy in a laser beam of limited duration (pulse or chopped), and  $\Delta U_{\text{el}}$  is the energy of an electrical calibration.

The change in internal energy of the calorimeter is the quantity  $E(T_f - T_i)$ ; the integral term evaluates the heat exchange. The subscripts  $i$  and  $f$  refer to initial and final measurements. The various terms are illustrated by the temperature-time curve in figure 2-2 for a hypothetical experiment. The parts of the curve preceding  $t_i$  and following  $t_f$  are single exponential functions of time used to evaluate  $\epsilon$  and  $T_{\text{surr}}$  in eq (8). The initial temperature,  $T_i$ , is read at  $t_i$  and the final temperature,  $T_f$ , is read at  $t_f$ . When the temperature is a single exponential function of time, these observations are a measure of the internal energy of the calorimeter. The internal energy so obtained is independent of the location of the source. If the integral term in eq (7) could be made negligible, the comparison of different sources therefore would be very accurate. This reasoning is applied in thermochemistry to make measurements to one part in 10,000 with a heat exchange of one part in 100. So far laser calorimeters come nowhere near this precision partly because the heat exchange is large relative to the internal energy of the calorimetry.

The integration in eq (8) can be done in a variety of ways to obtain the heat exchange over the time of the experiment. As it stands,



9'393

Figure 2-3.  $H_1$  and  $H_2$  are calibrating heaters; A is the control heater; S is a 20 junction thermopile; C is a resistance bridge for temperature control; and T is a copper resistance thermometer for monitoring the temperature.

this evaluation requires that the laser beam and the calibration energy have the same geometric distribution in the calorimeter. This unrealistic restriction can be removed by showing experimentally that the energy equivalent,  $E$ , is independent of the location of the energy input. Such independence can be designed into the calorimeter, using the idea of equivalent sources<sup>(4)</sup>. Briefly, the idea is to make the heat reach the surface of the calorimeter by the same path no matter what the energy distribution inside the calorimeter. An application is discussed in the next section.

By the technique of equivalent sources, the heat exchange can be properly accounted for. Since the internal energy,  $E(T_f - T_i)$ , is intrinsically independent of the source, the entire measurement is independent of the source, and provides an accurate means of comparing laser and electrical energies. Equations (8) and (9) therefore represent a complete theory of measurement, prescribing how an unknown quantity,  $\Delta U_L$ , is to be determined from temperature observations and a calibration experiment. Measured in this way, the energy in the laser beam is obtained ultimately in terms of the electrical standards maintained by the National Bureau of Standards. This direct relation to the electrical standards seem much preferable to reliance on the traditional radiometric standards.

### 2.1. An Application of the Theory

A calorimeter applying the principles set forth above is shown in cross-section in figure 2-3. The calorimeter accepts radiation on two polished conical surfaces which reflects the light into annular spaces where it is absorbed by multiple reflections. The calorimeter is surrounded by a thick aluminum block which has a heater and resistance thermometer for temperature control. The assembly is housed in an aluminum box.

Table 2-2

Dependence of Calibration Factor on Heater Location

Heater No. 1	Heater No. 2
.1150	.1107
.1144	.1103
.1143	.1107
.1146	.1106
	.1116
	.1112
Ave..1146	Ave. .1109
s = .0003	s = .0005

The calorimeter shows the application of the principle of equivalent sources. To reach the outer surface of the calorimeter (outer heavy line), heat flows from the heat or absorbing surface back to the ring, R, and then out to the calorimeter surface. This is an approximation, of course, since some heat can flow directly to the surface by radiation and air conduction.

Two heaters are installed to test the design. With the design as shown in figure 2-3, the results in table 2-2 were obtained for two series of calibrations ( $s$  is the estimated standard deviation.) Note that the reproducibility is excellent for each heater alone, but the systematic error implied by the different results is far poorer, showing that the two heater sources are not equivalent at the 1% level.

Another thin metal surface was placed around the calorimeter, attached only at the ring and spaced about  $1/8$  in. from the outer surface shown. A greater space would have been preferable, but would have required extensive modification of other parts. The calibrations were repeated with the following results: For heater number 1, average 0.1383,  $s = 0.0004$ ; for heater number 2, average 0.1364,  $s = 0.005$ ; difference 1.4%. Apparently, the added surface made the two sources more nearly equivalent.

The actual time-temperature curves for the two heaters are shown in figure 2-4. The energy inputs were equal, but the heat exchange was quite different for the two experiments, so that the amplitude of the final single exponentials are quite different. The solid curve extrapolates to the circle at zero time and the dashed curve to the cross, illustrating the error possible in data analysis by extrapolation on the assumption that the geometrical distribution of the two sources is the same. The difference is more than 5%.

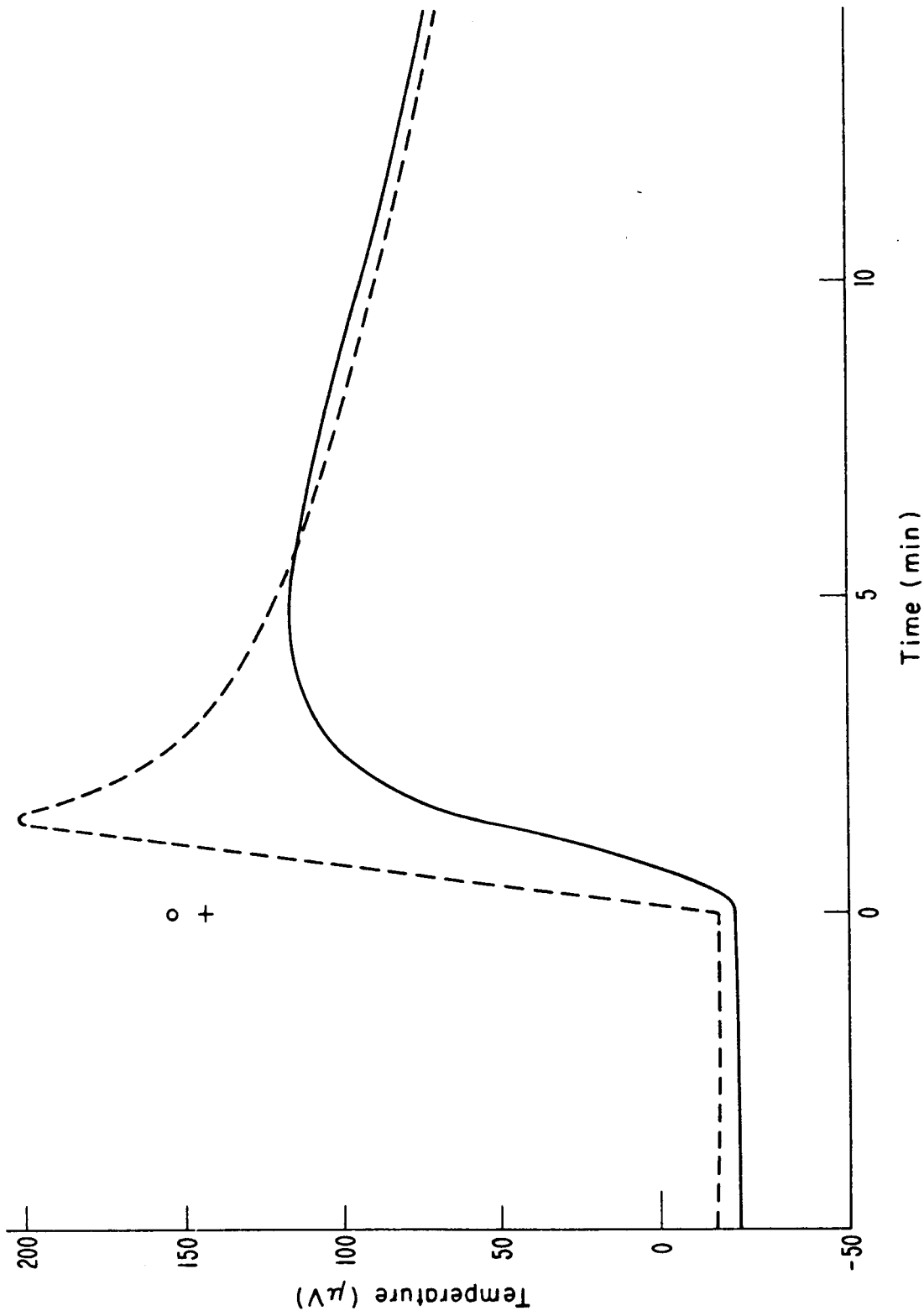


Figure 2-4. Temperature-time curves for different calibrating heaters on the calorimeter.

Another interesting point arises in connection with the constant temperature surroundings. The theory eq (3) requires constancy, but practically, the question is how constant? In this case the temperature of the calorimeter was measured by a thermocouple (S, fig. 2-3) relative to the surroundings. If the latter varied, the observed temperature was in error by the magnitude of the variation. For a 1 mK variation in a 0.1 K temperature rise, the error would be 1%. A temperature measurement independent of the temperature of the surroundings would give a smaller error because only the heat exchange would be affected.

#### References

1. L. M. Branscomb, *Scientific Research* 3 No. 11, p 49, May 27, 1968.
2. J. M. Cameron and Harmon Plumb in a talk given before the Society of Automotive Engineers, New York, April 21-24, 1969.
3. D. C. Ginnings in *Experimental Thermodynamics I*, J. P. McCullough and D. W. Scott, ed., Plenum Press, New York, 1968.
4. E. D. West and K. L. Churney, (To be published).
5. E. D. West and K. L. Churney, *J. Appl. Physics* 39, 4206 (1968).

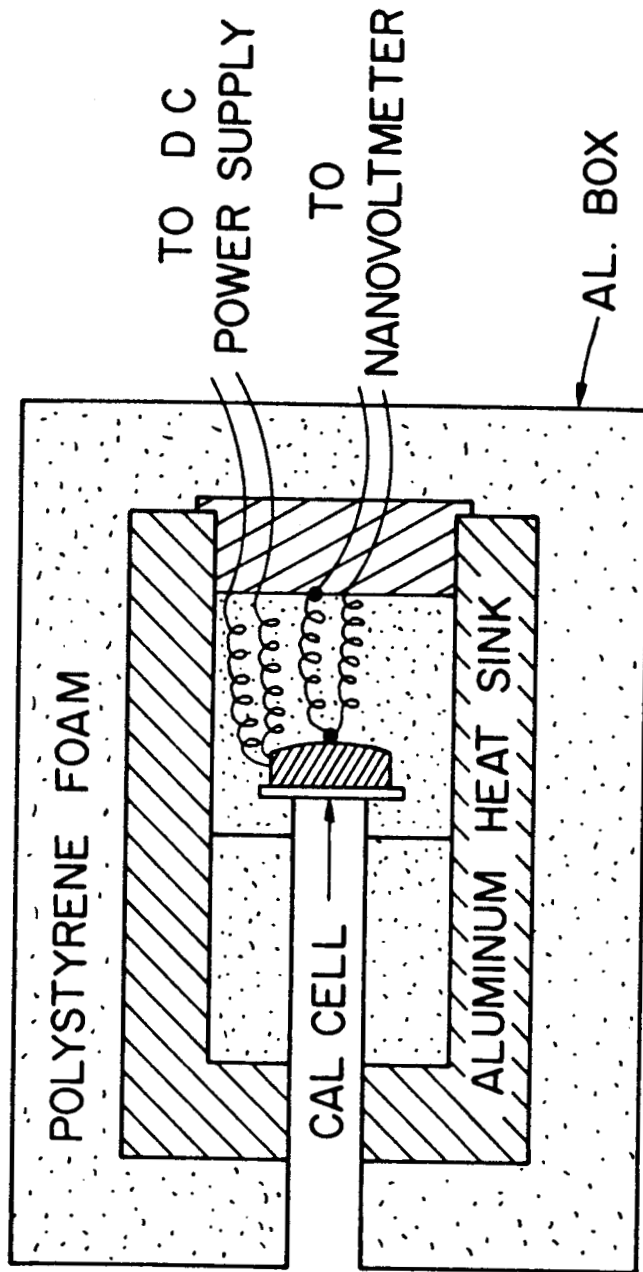


Figure 3-1. Cross-sectional diagram of the calorimeter, showing layout of components, method of insulating and supporting calorimeter absorption cell and position of the thermocouple.

94394



### 3. Energy Measurements

#### 3.1. Introduction

Of the several methods one may use to measure pulsed laser energy,<sup>1-8</sup> the calorimetric one is capable of yielding relatively high accuracy. We have designed, built and calibrated calorimeters for measuring the output energy of the pulsed ruby laser 694.3 nm and the pulsed neodymium laser 1060 nm. Input energy measurements 0.1J to 100J, to calibrate laser energy detectors, have an estimated  $\pm 2\%$  uncertainty. Energy measurements of our absorption cell calorimeters agree within 1% of our own reflecting metal plate calorimeters which absorb a known portion of the energy and reflect the rest.

Details are given in reference 8. They are reviewed here and modified according to the additional work accomplished.

#### 3.2. The Calorimeter

The calorimeter is shown in figure 3-1. The calorimeter absorption cell, filled with an energy absorbing solution, is supported in an aluminum or brass heat sink by polystyrene foam. The heat sink is also placed in low density polystyrene foam insulation and the entire system enclosed in an aluminum box. One junction of a copper-constantan thermocouple is attached with silver epoxy to the absorption cell, and the other junction is attached to the heat sink. The cell junction should have close thermal contact with the cell. When pulsed laser energy is fired into the absorption cell, the cell rises in temperature and the thermocouple generates a voltage proportional to the temperature difference between the absorption cell and the heat sink. The decaying output voltage of the thermocouple, logarithmically extrapolated to a reference time (see section 6 on calibration), is a measure of the energy

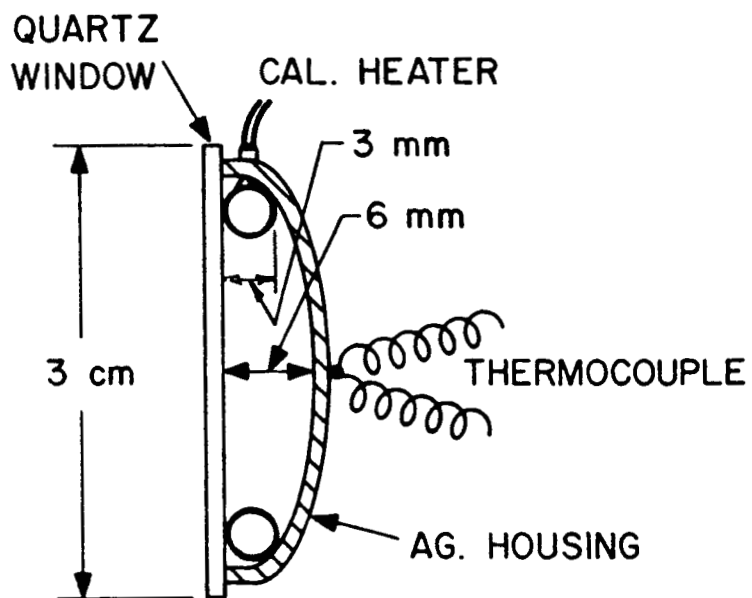


Figure 3-2. Cross-sectional diagram of the calorimeter absorption cell, showing the approximate size of components and the position of the heater wire.

in the laser beam. The extrapolation is made when the decay is a single logarithmical function. The voltage generated by the thermocouple is measured with a nanovoltmeter whose output is amplified and fed into a strip chart recorder.

A cross-sectional view of the absorption cell is shown in figure 3-2. The cell wall is made of silver  $\sim 0.5$  mm thick. The cell has a diameter  $\sim 3$  cm and a depth of 3 mm at the edge and 6 mm at the center. It has two or three small holes near the edge. One hole is utilized for filling liquid and the other one or two is for the heater wires. The latter has a Teflon coating, a resistivity of 16 ohms/foot and a total resistance  $\sim 100$  ohms. The entrance window is high optical quality quartz. A cement, used to bond materials with dissimilar expansivities, bonds the quartz window to the silver cell. A small amount of beeswax and cement is used to seal the fill and heater wire holes. The cell is filled with a one molal solution of  $\text{CuSO}_4 \cdot 5\text{H}_2\text{O}$ . A 4 mm air bubble between the heater leads relieves expansion of the heated liquid. The addition of a few drops of Bendix purple ink into the solution extends the useful range to  $< 500.0$  nm. The absorption characteristic of the solution is nearly the same at 694.3 nm and 1060.0 nm, although there is a large increase in it between these two wavelengths. The cell filled with this solution will absorb  $> 99.9$  percent of the laser beam, not including the Fresnel reflection at the entrance window which is 3.5%. The index of refraction of the glass and liquid are approximately the same.

The cell gives about  $0.1^\circ\text{C}$  temperature rise for a 1.4J input.

### 3.3. Methods of Calibration

Three independent methods of calorimeter calibration are used. One calibration is based on the thermocouple calibration ( $\mu\text{V}/^\circ\text{C}$ ) .

divided by the heat capacity of the absorption cell ( $J/^\circ C$ ); and the second, on the thermocouple output ( $\mu V$ ) divided by a dc electrical energy input (J) into the absorption cell heater; and the third, intercomparing at 694.3 nm to several reflecting metal plate calorimeters. A plate absorbs 43% of the energy and reflects the rest at a  $45^\circ$  angle into a liquid cell calorimeter. A correction is made for Fresnel reflection at the entrance window of the liquid cell and the absorption of some of this reflected energy by the plate.

Other details are also given in section 6.

#### a. Heat Capacity Calibration

The heat capacity calibration ( $\sim 3\mu V/J$ ) consists of the thermocouple calibration divided by the heat capacity of the absorption cell. All the component parts of the absorption cell are weighed and the most accurate obtainable values of the specific heats are used to calculate the heat capacity of the absorption cell. The largest part of the heat capacity is the heat capacity of the  $CuSO_4$  solution<sup>9</sup>. The thermocouple sensitivity is determined (error  $\pm 0.2\%$ ) by a technique described by Sparks and Powell<sup>10</sup>. Correcting for Fresnel reflection, the corrected specific heat calibration  $SHC_t$  compared to the calculated value  $SHC$  is  $SHC_t = SHC (1-R)$  where  $R$  is the reflectivity of the window.

#### b. DC Electrical Energy Calibration

The dc electrical energy substitution calibration is accomplished by applying energy  $J$  from a dc voltage  $V$  across the resistance  $r$  of the heater wire for a time  $t$  where  $J = \frac{V^2}{r} t$ . Corrections are made for the voltage drop and resistance of the cable to the heater. The calibrated value is obtained by making a logarithmical extrapolation of the thermal decay to a reference time (see section 6). The thermal output ( $\mu V$ )  $(1-R)$

is divided by the J input. Calibration value R here is the reflectivity of the window. The thermocouple output is normalized at 25° C. A ribbon thermometer attached to the heat sink is used to measure the temperature of the system. The thermocouple output is corrected for this temperature.

During the electrical calibration the gate output from a preset scaler, counting the line frequency (60 Hertz), is used to turn on a transistor switch. The transistor is powered by a constant current source (constant to 0.01%), and the absorption cell heater wire is in the collector circuit of the transistor. The voltage drop across the heater is monitored by a digital voltmeter and a calibrated strip chart recorder. A recorder event mark determines the starting time.

#### c. Reflecting Plate Calibration

Intercomparison of liquid cell calorimeters to reflecting metal plate calorimeters yield energy values within 1% from each other. The reflecting plate is calibrated from the thermocouple calibration and the heat capacity and reflectivity of the plate. It reaches a uniform temperature in 2 or 3 seconds. The laser energy is the  $\mu\text{V}$  output divided by the calibration value. A detailed discussion is given later.

#### 3.4. Logarithmical Extrapolation

Logarithmical extrapolation of data may be accomplished as follows. One may plot the  $\mu\text{V}$  output versus time on semilog paper. The output coordinate is the log scale and the time is the linear scale. The straight line portion of the curve when a single logarithmical decay occurs, is extrapolated to find the  $\mu\text{V}$  output  $y_T$  at a reference time (see section 6). In a second method two points are selected from the portion of the curve where a single logarithmical decay occurs. An extrapolated

output is calculated using the expression for  $y_r$ . If the same two points are always used, precision is improved for those calorimeters whose decay deviates slightly from a single logarithmical function. We have for the output  $y_r$  at  $t_r$

$$y_r = y_1 e^{t_1/\tau} \quad (1)$$

$$\tau = \frac{t_2 - t_1}{\ln(y_1/y_2)} \quad (2)$$

where  $y_1$  and  $y_2$  are the  $\mu\text{V}$  output at  $t_1$  and  $t_2$ . For the NBS calorimeters,  $\tau \approx 1000$  seconds,  $t_1 = 240$  sec and  $t_2 = 600$  sec. The chart paper is centimeter cross section with millimeter divisions and 25 centimeter width. Chart speeds of 1.25 cm/minute or greater are used. To maintain accuracy, half to full scale deflection of  $y$  is used. To calculate  $y$  values, prefiring data at a constant or zero slope is used as a baseline. All data are read to  $\frac{1}{10}$  of a division.

The upper bound on the percentage error of  $y_r$  for no error in time is

$$\frac{|dy_r|}{y_r} = \left( \frac{1}{t_2 - t_1} \right) \left( t_2 \frac{|dy_1|}{y_1} + t_1 \frac{|dy_2|}{y_2} \right). \quad (3)$$

Using several output values on the decay curve, the value of  $y_r$  deviates ( $\sim 0.1\%$ ) from data using only  $y_1$  and  $y_2$ .

Let us briefly consider extrapolation in calibrating a calorimeter with a relatively long time constant and large thermal capacity. Sometimes linear extrapolation to a reference time or a maximum of the output voltage of the unknown is used. This leads to errors which can be ~10% when the area of the beam's cross-section and/or the magnitude of the beam changes. Logarithmic extrapolation to a reference time gives a calibration independent of the beam area or intensity for the range of the instrument. The maximum output voltage gives a precise calibration factor for fast responding calorimeters.

### 3.5. Intercomparisons Using Liquid Cell Calorimeter

To intercompare calorimeters and other detectors at 694.3 nm, we use the apparatus arrangement shown in figures 3-3, 3-4, and 3-5. We evaluate the energies received  $E$  and the reflectivities  $R$ . These are approximately 4%, 20% and 40% for  $R_4$ ,  $R_{20}$  and  $R_{40}$ , respectively.  $R_4$  can be used for making measurements from ~20 to 100 J;  $R_{20}$ , 5 to 20 J; and  $R_{40}$ , 1 to 5 J.  $R_4$  and  $R_{20}$  can also be used for measuring energies < 1 J. To know the laser energy one might expect for measurements, the laser output is calibrated ~10%.  $R_4$  and  $R_{20}$  are used together because of the maximum energy limits of the NBS calorimeter.

The energy input to the unknown device,  $E_u$ , is evaluated after determining the energies received and the reflectivities of the components in figure 3-3 and figure 3-4. The calorimeters and beam splitters are 1 to 2 meters from the output mirror of the laser.

We have

$$E_N = \frac{\mu V(\text{output laser energy})}{\mu V(\text{output dc energy}) (1-R)/J(\text{dc energy})} \quad E_N \text{ is the energy of an NBS calorimeter.}$$

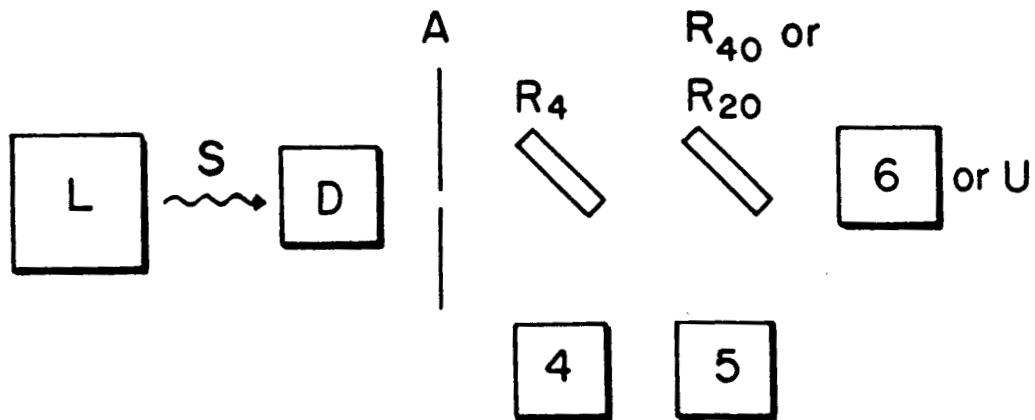


Figure 3-3. Block diagram of apparatus arrangement used to inter-compare pulsed laser energy measuring devices. Laser L, demagnifier D, aluminum oxide porcelain aperture A, NBS calorimeters 4, 5, 6 and device U, and beam splitters  $R_4$ ,  $R_{20}$  and  $R_{40}$  with reflectivities 4, 20, and 40%, respectively. D reduces the diameter of laser beam to  $\sim 1/4$  size.  $A = 3/8''$ , etc., depending on devices to be calibrated.

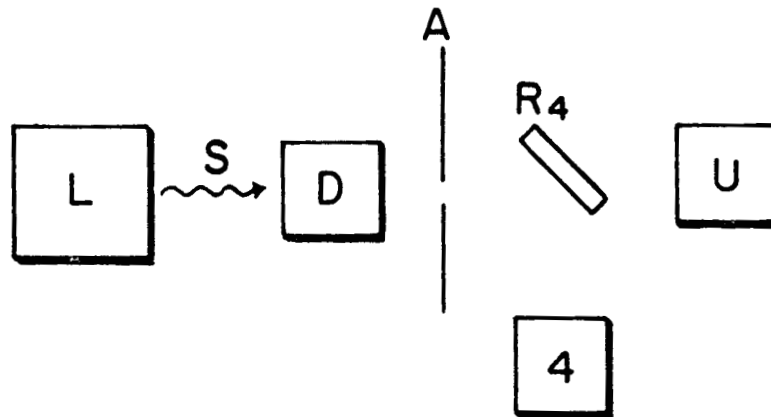


Figure 3-4. Same as figure 3-3 with the second beam splitter removed.



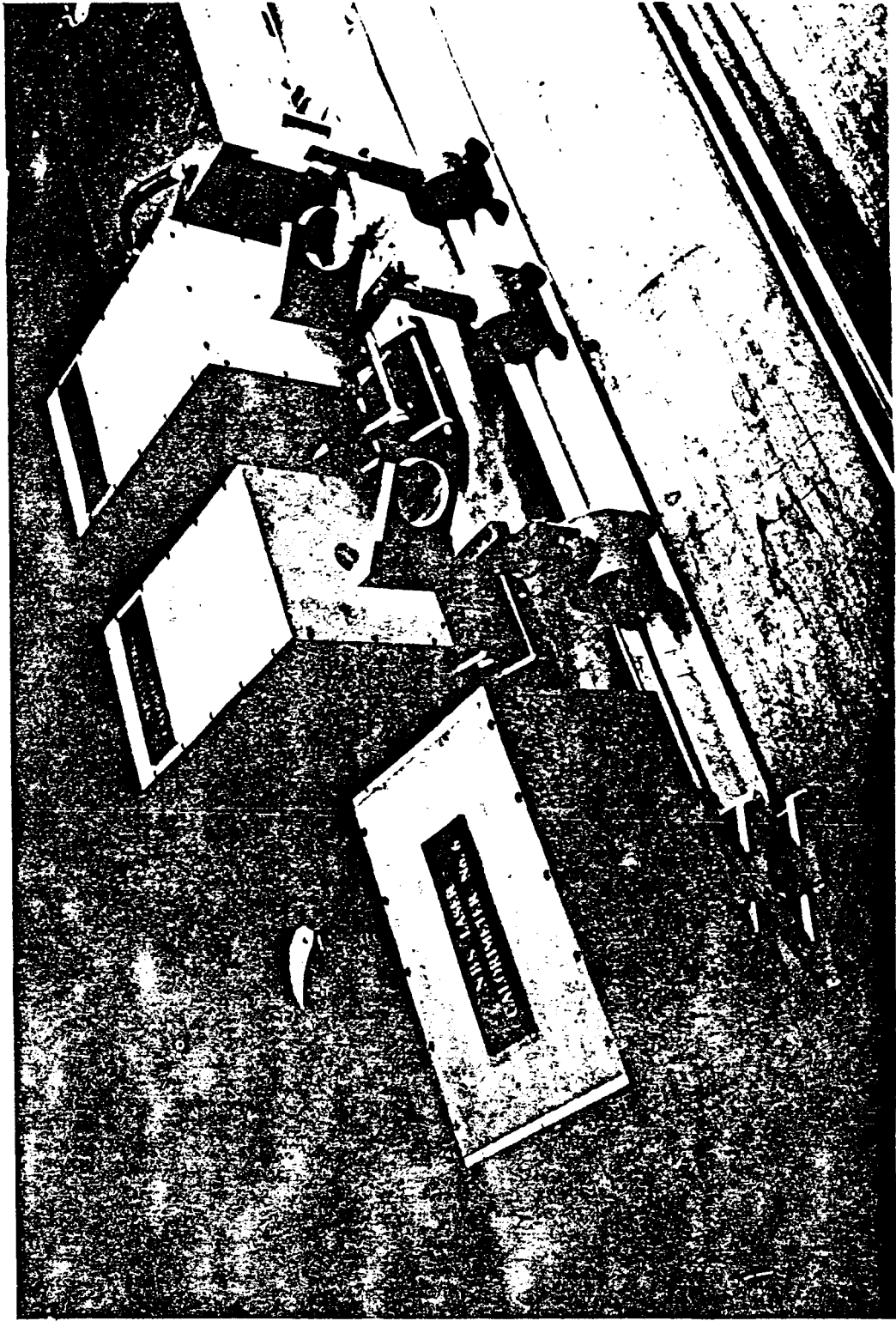


Figure 3-5. Photograph of apparatus arrangement of figure 3-3 with Laser L and demagnifier D not showing.

$$R_{20} = \frac{E_5}{E_5 + E_6}$$

See figure 3-3 for laser output S. Calorimeter 6 used.

$$R_4 = \frac{E'_4}{\frac{E'_5}{R_{20}} + E'_4}$$

See figure 3-3 for laser output S'. Device U used.

And

$$E''_u = \left( \frac{1 - R_4}{R_4} \right) E''_4 = \frac{E'_5}{\left( \frac{E_5}{E_5 + E_6} \right) E'_4} E''_4$$

See figure 3-4 for laser output S''.

Since  $E_6 \approx 4E_5$ , the error of  $E''_u$  is approximately the error of  $E_6$ .

When  $R_{20}$  or  $R_{40}$  are used to determine the energy  $E_u$ , we have

$$E'_u = \left( \frac{1 - R_{20}}{R_{20}} \right) E'_5, \quad \text{for } R_{20}.$$

or

$$E'_u = \left( \frac{1 - R_{40}}{R_{40}} \right) E'_5, \quad \text{for } R_{40}.$$

And

$$E'_u = \frac{E_6}{E_5} E'_5, \quad \text{where } \frac{E_6}{E_5} \text{ for } R_{20} \neq \frac{E_6}{E_5} \text{ for } R_{40}.$$

Again the error of  $E'_u$  is approximately the error of  $E_6$ .

Using  $R_4$  and  $R_{20}$  to calibrate a calorimeter gives values which agree within 1%. Using  $R_{20}$  and  $R_{40}$  to calibrate another calorimeter gives similar agreement. The NBS calorimeters need to be recalibrated occasionally to check the absorption cells for leakage.

At 1060 nm the same setups are used except the reflectivities of the beam splitters  $R_{44}$  and  $R_6$  are 44% and 6%. These are used similarly to  $R_{20}$  and  $R_4$  in calibrating for measurements at relatively high energies at 1060 nm.

If the position of the unknown and the NBS calorimeter are interchanged in figures 3-3 and 3-4 then energies below 1 J can be measured.

The estimated calibration uncertainty over the energy range is  $\pm 2\%$ . The energy  $E_N$  of an NBS calorimeter is

$$E_N = \frac{\mu V(\text{output laser energy})}{\mu V(\text{output dc energy}) (1-R)/J (\text{dc energy})}$$

If the same nanovoltmeter and recorder are used with a given calorimeter without changing the instrument ranges, no error occurs in the output voltage ratio above. Its precision is ( $\sim \pm 0.2\%$ ). The estimated error in the dc energy J is ( $\sim \pm 0.1\%$ ). The estimated error from the substitution of dc energy for laser energy is ( $\sim \pm 0.1\%$ ). The estimated calibration error of the nanovoltmeter is ( $\sim \pm 0.1\%$ ), the recorder is ( $\sim \pm 0.1\%$ ) and the reflectivity ( $R \sim 40\%$ ) is ( $\sim \pm 0.2\%$ ). For reflectivity ( $R \sim 5\%$ ), it is ( $\sim \pm 0.5\%$ ). A Lindeck potentiometer made from NBS and commercial components is used to calibrate the voltmeters and recorders.

### 3.6. Intercomparisons Using Metal Reflecting Plate Calorimeter

Liquid cell and reflecting metal plate calorimeters are intercompared at 694.3 nm. They agree with each other within 1% over an

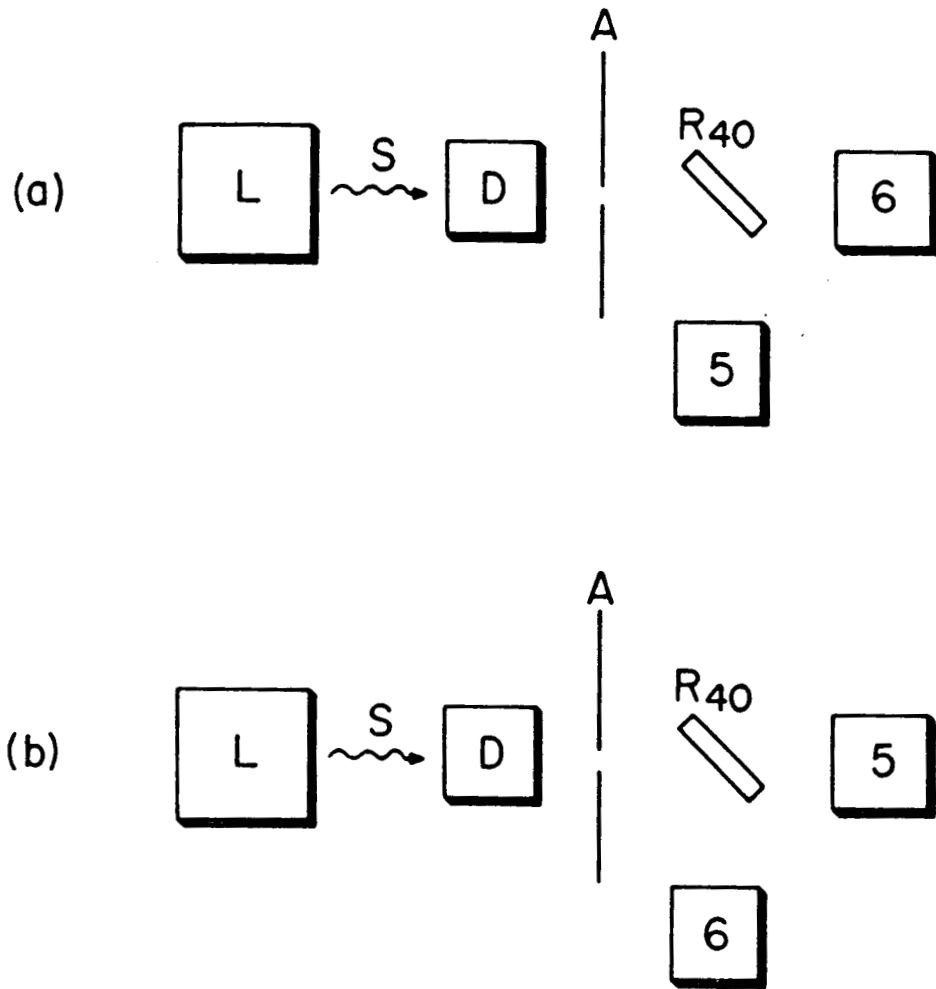


Figure 3-6. Setup to calibrate  $R_{40}$ . Refer to figure 3-3 for identification of symbols.

input energy range of several joules. The plate absorbs 43% of plane polarized light and reflects the rest at 45° angle into a liquid cell calorimeter. The plate is a 99.9% purity silver disk, diameter 1-1/2" and thickness 0.17". It is optically polished being relatively free of imperfections and plated with 99.5% purity nickel 10-15 · 10<sup>-6</sup> inch thick. The purpose of the plating is to increase the sensitivity and precision of measurements. The plate reaches a measured uniform temperature in 2 or 3 seconds. Two calibrated thermocouples are mounted at the center and edge of the back of the plate using a low temperature Indium alloy solder. The plate is housed similarly to the liquid cell calorimeter except there are both an entrance and an exit.

Laser energy  $E_L$  is determined from the absorbed energy of the plate  $E_p$ , the reflectivity of the plate  $R_p$  (calibrated from measurements using the liquid cell calorimeters) and a correction for plate absorption of some of the energy reflected from the liquid cell calorimeter. This latter energy is two percent of the energy absorbed by the plate.  $E_p$  equals the  $\mu V$  rise in temperature at the time of energy input divided by the heat capacity calibration of the plate ( $\sim 3.5 \mu V/J$ ).

We have for the laser energy

$$E_L = \frac{E_p}{(1 - R_p)(1 + R_p R'_6)}$$

where  $R_p R'_6 = 0.020$  to a close approximation.

To make inter-comparisons of the two types of calorimeters the following measurements are made.

The absolute value reflectivity of  $R_{40}$  is measured using the setup shown in figure 3-6. Using setup (a),  $E_5$  and  $E_6$  are measured.

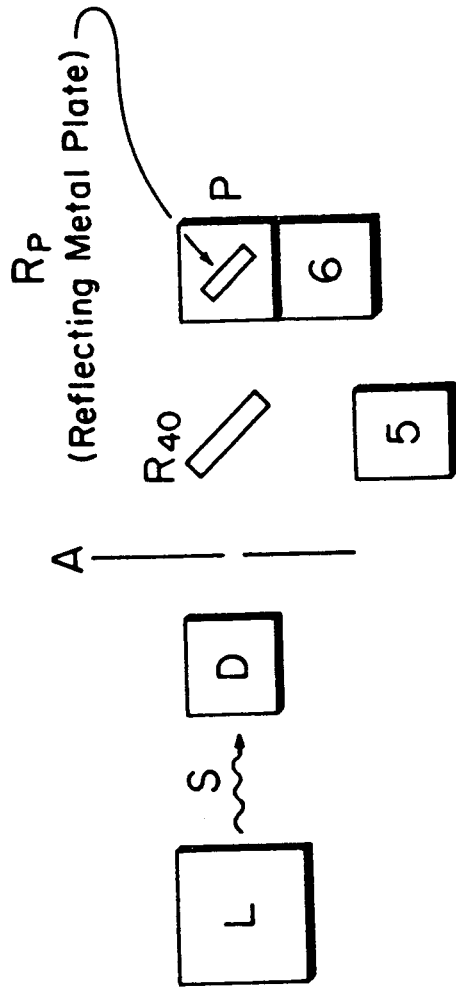


Figure 3-7. Setup to intercompare liquid cell and reflecting plate calorimeters. P is a reflecting plate calorimeter. Refer to figure 3-3 for identification of other symbols.

Calorimeters 5 and 6 are the liquid cell type. Using setup (b),  $E'_5$  and  $E'_6$  are measured, where

$$R_{40} = \frac{\frac{E_5}{E_5 + E_6} + \frac{E'_6}{E'_5 + E'_6}}{2}$$

Average of several sets of data is used to find  $R_{40}$ .

The reflectivity  $R_p$  of the reflecting plate is measured using the setup shown in figure 3-7.  $E_{5p}$ ,  $E_{6p}$  and  $E_p$  are measured

$$R_p = \frac{E_5}{E_6} \frac{E_{6p}}{E_{5p}}. \text{ Average of several sets of data is used to find } R_p.$$

To intercompare calorimeter 6 with calorimeter P, we use the following expression

$$E_{6p} = \left( \frac{R_p}{1 - R_p} \right) \left( \frac{E_p}{1 + R_p R_6} \right)$$

And for calorimeter 5, we have

$$E_{5p} = \left( \frac{R_{40}}{1 - R_{40}} \right) \frac{E_p}{(1 - R_p) (1 + R_p R_6)}.$$

The error of  $E_p$  is ( $\pm 0.5\%$ ). The error of the reflectivities are approximately as given in the previous section.

### 3.7. Other Parts of the System

Let us consider other parts of the system. The ruby rod has its crystal axis aligned horizontal  $\sim \pm 1^\circ$ . The outputs of the ruby and neodymium rod lasers are plane polarized light. Polarizers are used with the neodymium laser because its output is unpolarized without them. They must thoroughly polarize the light so that the reflectivity will not vary as a function of the intensity of the laser beam. Both lasers are aligned with their beams parallel to the optical bench at a constant elevation above it. The demagnifier reduces the beam to about  $1/3$  to  $1/4$  size. It is adjusted to give a beam with approximately parallel rays. If the rays converge, they will yield destruction where they are most concentrated. The beam splitter is sensitive to change in its angle with respect to the laser. If any part of the system moves, the calibration of the beam splitter changes. Consequently, the reflectivities of the beam splitters need frequent calibration. Movement of the calorimeters will affect the accuracy of measurements if not all the energy is captured.

To assure proper alinement of a calorimeter, an aluminum plug with cross hairs is placed in its entrance with a piece of photographic paper over it which burns a clear image. Glass covers are placed between the target and the beam splitter. The glass protects the latter from a searing heat wave. The calorimeters are aligned so that the burned area is close to the center of each entrance.

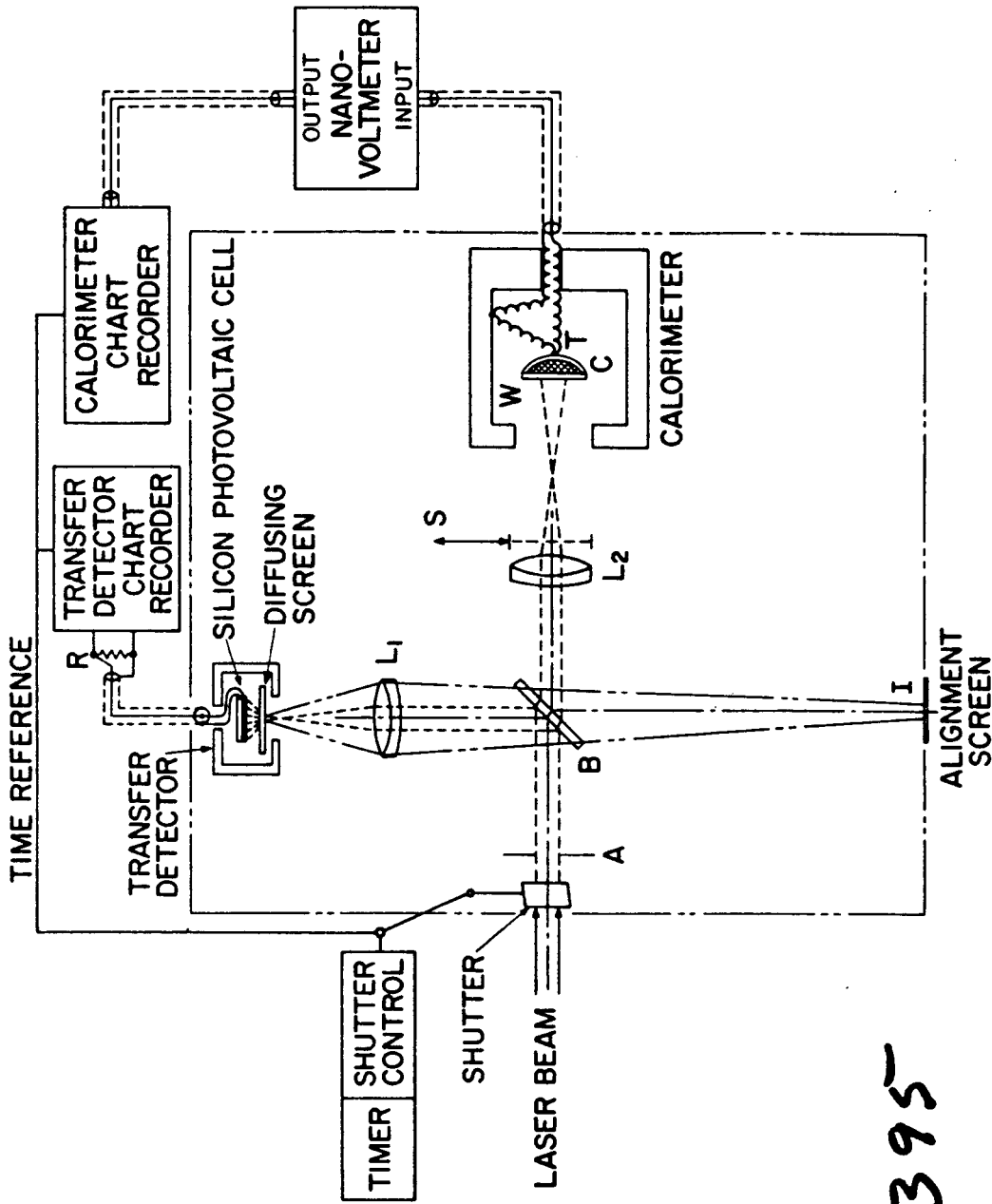
The beam splitters are 2" diameter,  $1/2$ " thick and 30 minutes of arc wedge. A reflective coating is on the front surface and an anti-reflective coating on the back surface from the laser. The beam splitters can withstand higher energy if they are used this way because the front surface needs to be able to yield when the laser pulse strikes it. The laser light is plane polarized in the horizontal direction. The



beam splitters are mounted vertically at a  $45^\circ$  angle. The same orientation is used in the reflecting metal plate calorimeter. The wedge of the beam splitter is adjusted for minimum horizontal deflection of the transmitted beam and for discarding the reflection from the back surface of the beam splitter. Energy data using several beam splitters indicate that the energy lost by absorption or scatter from them is negligible.

#### References

1. G. Birnbaum and M. Birnbaum, Proc. IEEE, 55, No. 6, 1026 (1967).
2. D. E. Killick, D. A. Batemen, D. R. Brown, T. S. Moss and E. T. DeLaPerrelle, Infrared Phys. 6, 85 (1966).
3. A. J. Schmidt and R. C. Greenhow, J. Sci. Instr. 44, 468 (1967).
4. J. G. Edwards, J. Sci. Instr. 44, 835 (1967).
5. H. S. Heard, "Laser Parameter Handbook," (John Wiley & Sons, New York, 1968), p 480.
6. R. A. Valitov, Yu. A. Kalinin and V. M. Kuz'michev, Translated from Izmeritel'naya Tekhnika, No. 5, 37 (May 1965).
7. A. V. Kubarev, A. S. Obukhov, A. Ya. Leikin, Y. S. Solov'ev and V. P. Koronkevich, Translated from Izmeritel'naya Tekhnika, No. 11, 20 (Nov. 1967).
8. D. A. Jennings, IEEE Trans. on Instr. & Meas. IM-15, No. 4, 161 (Dec. 1966).
9. A. F. Kapustinskii, B. M. Yakushevskii and S. L. Drakin, Zhur. Fiz. Khim., 27, 588 (1953).
10. L. L. Sparks and R. L. Powell, Measurements and Data, 1, 82 (1967).



94395

Figure 4-1. Schematic of the CW laser power meter calibration system.

## 4. CW Power Measurements

### 4.1. General Description

The need often arises while working with CW lasers for measuring the absolute power in the laser beams. The calorimeter used for pulsed laser energy measurements as described earlier lends itself to the task of absolute power calibration of power meters. Since the calorimeter and its associated equipment have already been calibrated, it can be used as a device to integrate the power of a CW laser beam for a measured period of time from which the average power can be determined. However, due to the necessity of using long integration times, on the order of 1 to 2 minutes, the heat losses from the calorimeter cell during the initial temperature rise are not the same as for pulse laser energy measurement. It is necessary therefore to use an electrical calibration pulse of the same power level and same time duration as the CW laser pulse.

A schematic representation of the CW laser power meter calibration used in this laboratory is shown in figure 4-1. The function of each component is as follows: the time-shutter control actuates the shutter and precisely controls the time during which the laser beam enters the unit. In addition it provides a time reference for the two chart recorders. The beam splitter, B, divides the beam into two parts; one part is directed towards the transfer detector and the other part illuminates the calorimeter cell, C. A diffusing screen is placed before the silicon photovoltaic cell in the transfer detector to provide more even illumination and to prevent damage of the photocell surface. Two recorders record separately the output of the transfer detector and the calorimeter as a function of time. The time reference is recorded on the second channel in each. R, which terminates the output

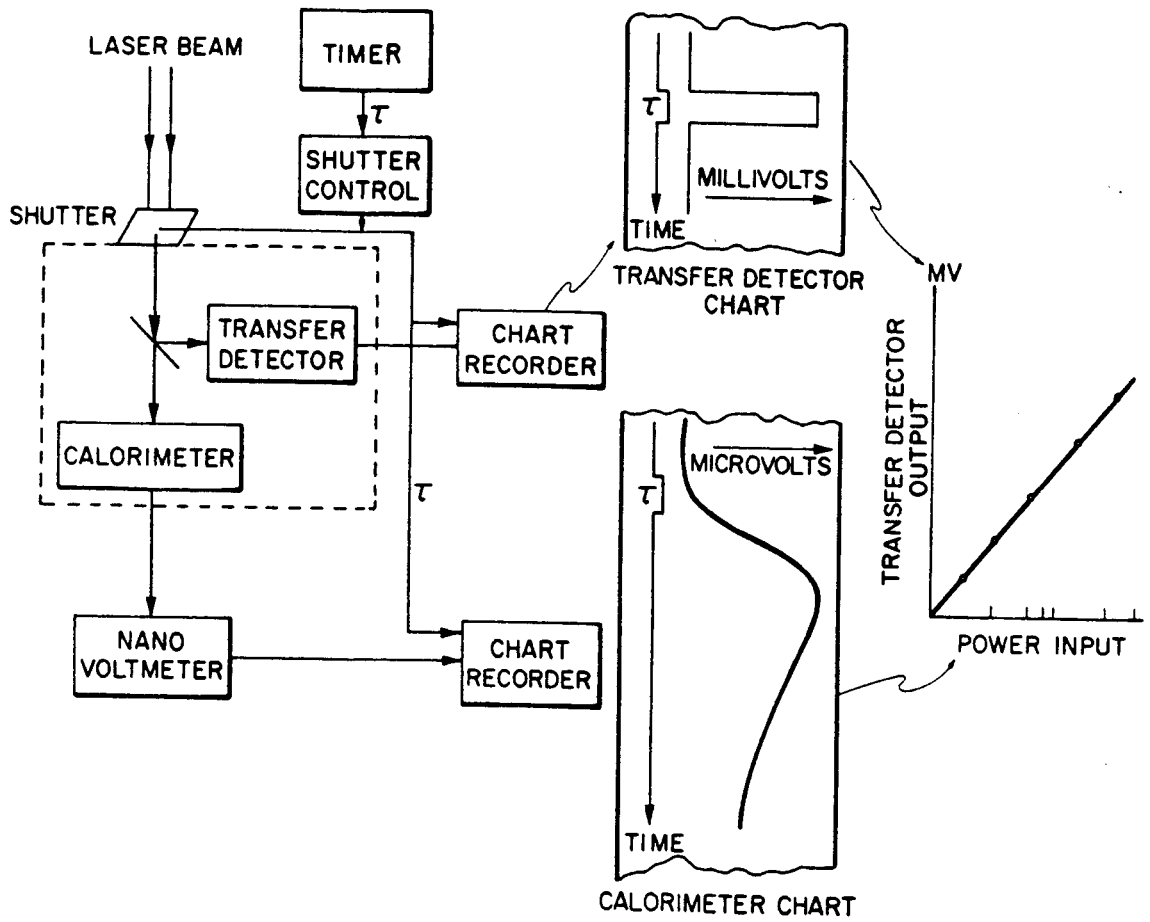


Figure 4-2. Diagram showing the basic calibration procedure.

of the transfer detector, is chosen such that the maximum illumination of the transfer detector will not produce a nonlinear output of the photocell. The achromatic lens,  $L_2$ , provides a divergent beam to accommodate power meter sensing heads with different diameter apertures. Lens  $L_1$  produces an image,  $I$ , on the alignment screen of the beam spot on the transfer detector. This provides a convenient means of checking the alignment of the calibration unit with respect to the incoming laser beam throughout the entire calibration.

The calibration procedure consists of two parts. In the first part the output of the transfer detector is calibrated in terms of absolute power in the laser beam as seen by the calorimeter. Schematically this is shown in figure 4-2. After the calibration unit has been aligned with the laser beam, the time is set for a time  $\tau$  and the shutter is activated. The output of the transfer detector in millivolts is recorded on one chart recorder as a function of time. Simultaneously the output of the calorimeter is recorded on the other recorder as a function of time. The reference time pulse on the transfer detector recorder provides a check of zero time and on the other it determines zero time.

The output of the calorimeter begins to rise with the onset of the laser beam and the light energy is converted to heat energy. It continues to rise after the shutter is closed until an equilibrium is reached after which the cooling is predominantly that due to Newton's law of cooling and hence fits an exponential decrease. Thus by using data points to fit an exponential and knowing the calibration constant (determined as described earlier) in microvolts per joule of the calorimeter, the total electromagnetic energy incident on the calorimeter for the time,  $\tau$ , can be determined.

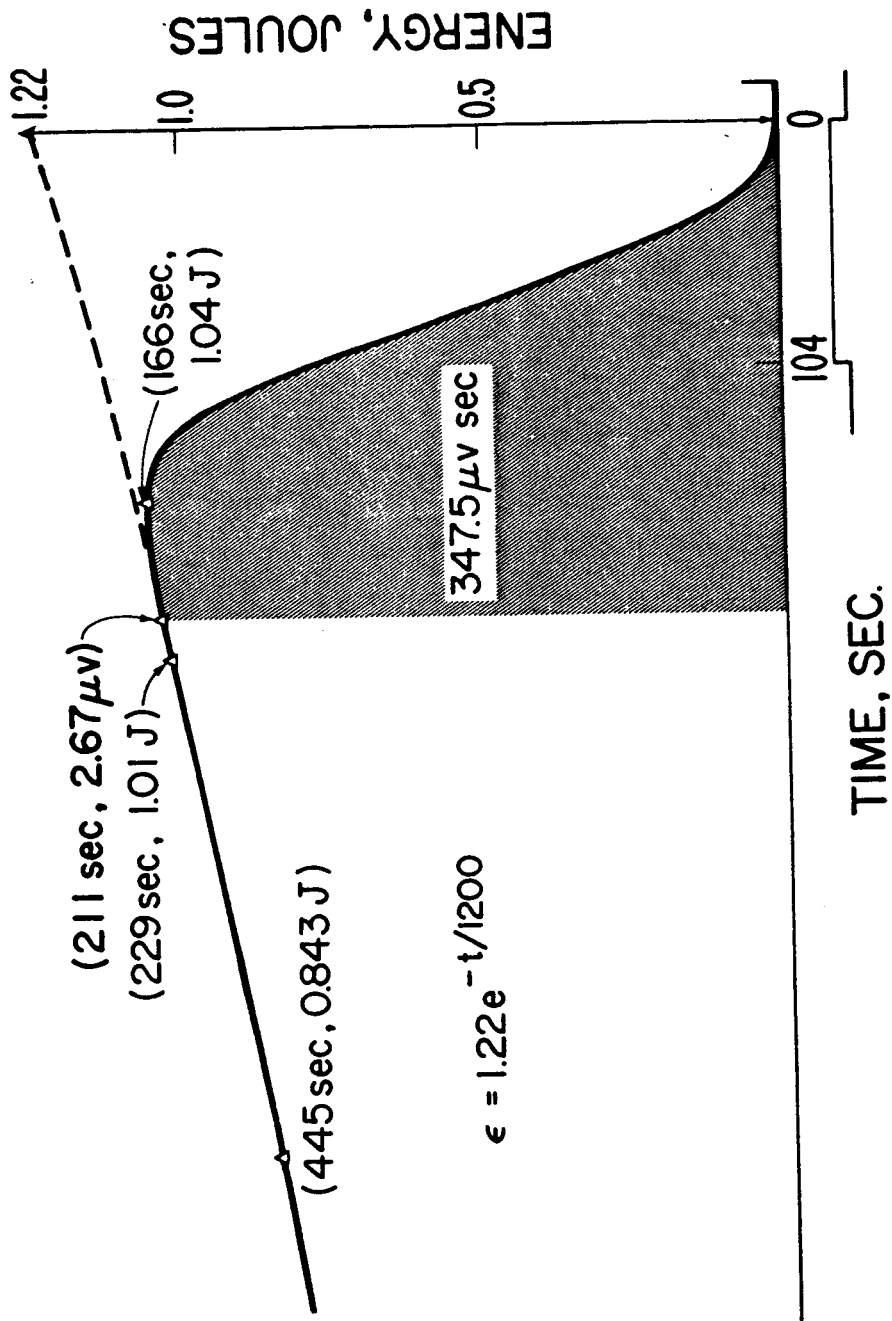


Figure 4-3. The response of the liquid cell calorimeter to a CW laser beam. The CW laser beam was interrupted by a timed shutter.

The average power then leaving lens  $L_2$  is known for one power level input. Repeating this procedure for other power levels into the calibration unit yields a straight line graph of millivolts output of the transfer detector as a function of the laser beam power leaving lens  $L_2$  for one wavelength.

The second and last part of the calibration is performed by replacing the calorimeter with the sensing head of the power meter to be calibrated. Since the output of the transfer detector is now calibrated in terms of the power incident on the power meter sensing head, it is merely necessary to compare outputs and the calibration is complete.

Figures 4-3 and 4 show data obtained during a power meter calibration. The three wavelengths used were 514.5 nm and 488.0 nm lines from an argon ion laser and the 632.8 nm line from a helium neon laser. Various power levels in the beam were obtained by varying the input power to the laser.

One of the calorimeter output recordings is shown in figure 4-3. The illumination was the 488.0 nm line. The two points shown are examples of the points used to determine the constants of the exponential cooling curve; the equation of which is also shown. The average power seen by the calorimeter in this case was 10.9 milliwatts as determined by the method discussed in section 6. (See section 6). Also indicated by the event marker is the time, 104 seconds, that the laser beam illuminated the calorimeter.

The results of the first part of the calibration procedure, namely calibration of the transfer detector are shown in figure 4-4. The values of the ordinates for the plotted points shown were obtained from curves like figure 4-3. Values for these data point abscissas were obtained from the output of the transfer detector as measured across a five ohm terminating resistor with a calibrated chart recorder. The chart re -

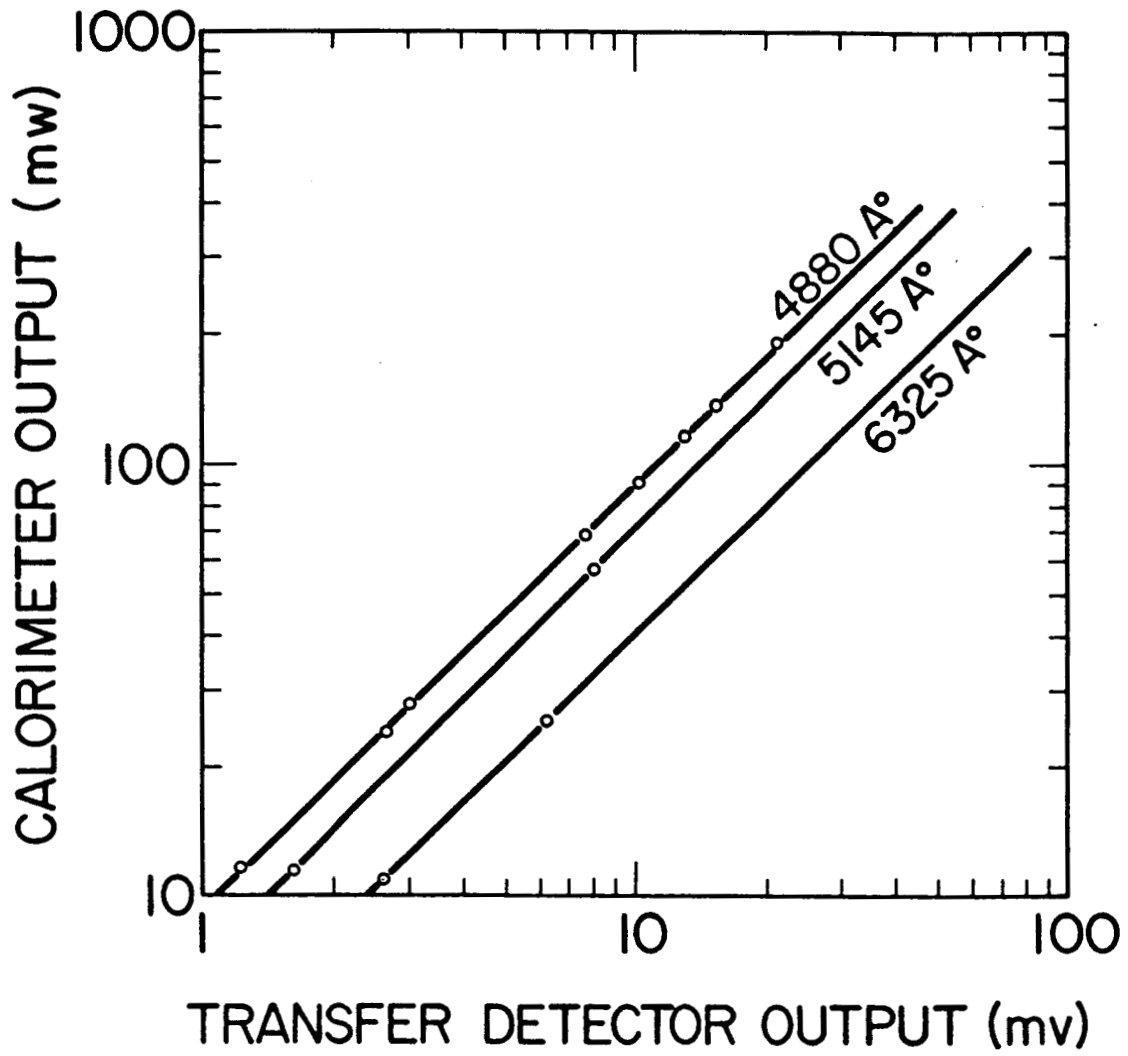


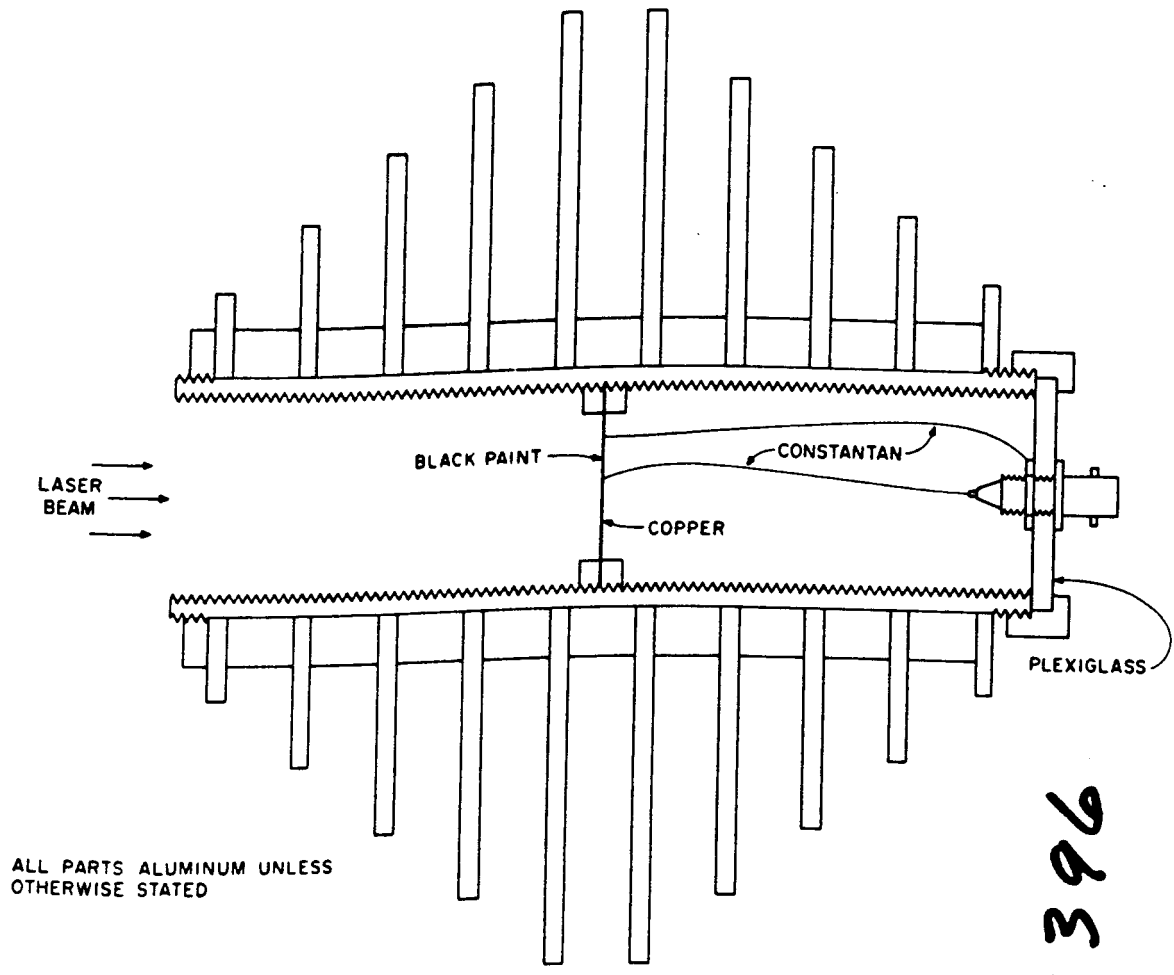
Figure 4-4. Transfer detector calibration as a function of laser power.



order also provided a monitor of the laser beam during the time of illumination. Since the curve for the 488.0 nm line was linear, it was assumed the curves for 514.5 and 632.8 nm lines would also be linear and only two data points were used.

The last part of the calibration was completed by replacing the calorimeter with the sensing head of the power meter and comparing the power meter readings with the curves of figure 4-4.

The estimated error in a single point on the curves of figure 4-4 is approximately  $\pm 4\%$ . This value was determined as follows. An estimated error of 1% is associated with the calorimeter--nanovolt-meter-chart recorder calibration. In fitting the exponential curve of figure 4-3, it is estimated that the coefficient of the exponential which is the energy into the calorimeter is determined to within  $\pm 1.3\%$ . The timer used here has an uncertainty for the shortest time of  $\pm 0.8\%$  plus a  $\pm 1\%$  uncertainty in the shutter activation.



94396

Figure 5-1. Schematic of the copper disc calorimeter showing construction details.

## 5. CW Power Measurements in Excess of 1 Watt

### 5.1. Introduction

The advent of lasers capable of producing many watts of power (notably the CO<sub>2</sub> laser) has produced a demand for methods of measuring these powers.

A simple method of measuring powers in excess of 1 watt consists of absorbing the laser beam in a calorimeter and measuring the heat produced. Several different types of calorimeters were tried and will be discussed. The most recent design will measure from 1 watt to 5 kilowatts with an accuracy of better than 3% at 100 watts. Although the calorimeter was used at a wavelength of 10.6 $\mu$ , it should work well throughout the visible spectrum.

### 5.2. Calorimeters

Three different calorimeters were used to measure the power of a CW 200 watt CO<sub>2</sub> laser. All three devices utilized standard calorimetric techniques to measure the heat produced by the absorption of the laser beam. The three devices, the disc, cone-disc, and cone-flow power meters will be described separately.

#### a. Disc Power Meter

A copper disc blackened with flat black spray paint served as the absorber in the disc power meter shown in figure 5-1. The reflectivities of various materials was measured by using a beam splitter arrangement and comparing the reflected intensities with that from a polished copper surface. The results are summarized in table 5-1. The heat absorbed in the central region of the disc flowed to the periphery of the disc and was dissipated by the cooling fins. The thermal gradient

Table 5-1.

Reflectivities of various materials at 10.6 microns compared with polished copper. (Accuracy about 10%).

Surface	Direct Reflection	Total Reflection (Direct & Diffuse)
Heavily anodized aluminum (undyed)	0.45%	3.5%
" " " (dyed black)	0.55%	3.7%
3-M velvet coating #101-C10 black	0.2%	6.0%
Aluminum anodized cone	< 0.2%	~ < 1%
Velvet coated cone	< 0.2%	~ < 1%
Aluminum oxide disc	0.94%	9.0%

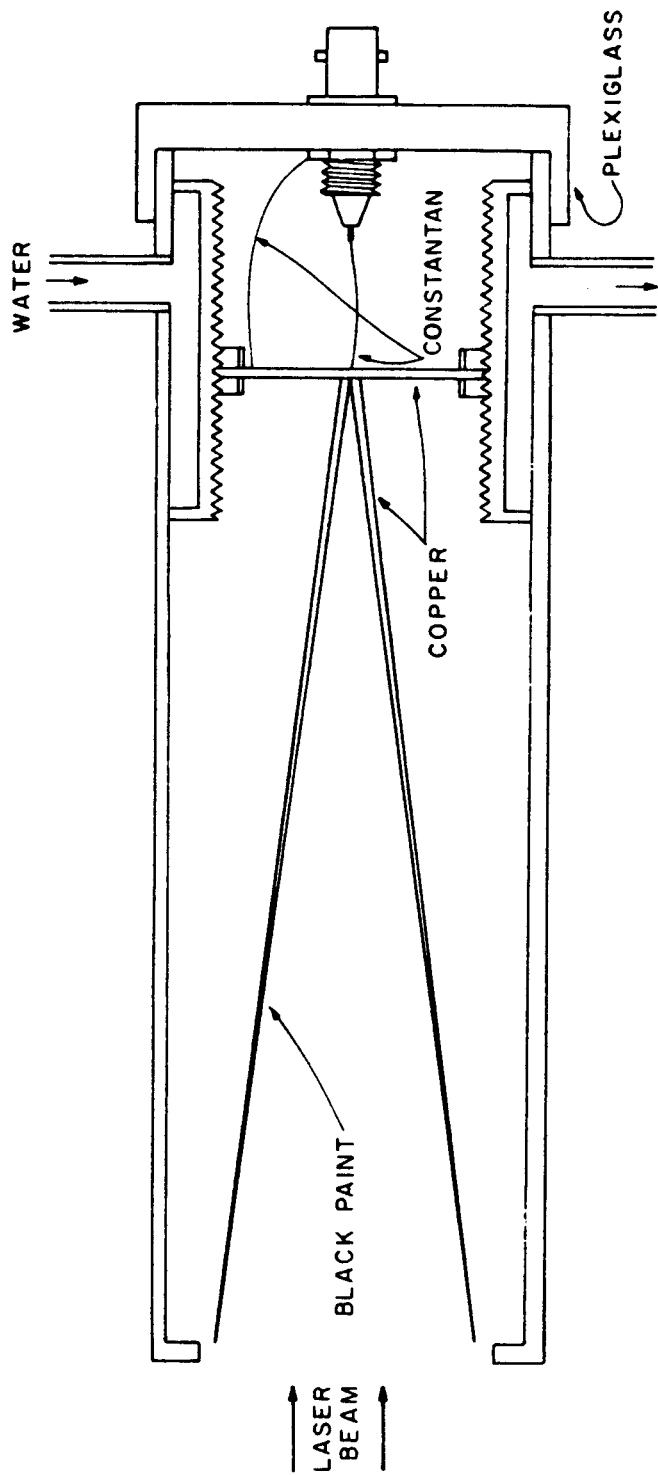


Figure 5-2. Schematic of the cone-disc power meter showing construction details.

on the disc was measured with a copper-constantan thermocouple with one junction at the center and one on the periphery. The device proved very useful and convenient for relative power measurements, partly because it had a shorter time constant than the other two calorimeters used (about 0.1 second). However, the disc became excessively warm during operation, and the output varied by several percent as the beam diameter and its position on the disc was changed, therefore no attempts were made at accurate calibrations of the disc power meter and it is presently used as a convenient relative power indicator.

#### b. Cone-Disc Power Meter

In the cone-disc power meter shown in figure 5-2, a blackened cone absorbs the laser beam and the heat then flows radially through a disc attached to the apex of the cone as in the disc power meter. The periphery of the disc is water cooled to lower the temperature of the device and thus lower the loss of heat due to radiation and convection. The cone serves to reduce reflection losses which may amount to 10 percent from the disc-power meter and to reduce the dependency on beam position and area. To calibrate this power meter, an insulated heater wire was wound on the outer surface of the cone and coated with conducting epoxy to distribute the heat. The electrical heat dissipation was plotted versus the thermocouple voltage from 25 to 150 watts. Three major flaws were noted early in the use of this power meter; the thermocouple output varied with the flow of cooling water, and the cone became warm enough to heat up the outer shield of the meter, and the response time was excessively long (several minutes). In spite of these drawbacks good agreement (2%) was obtained at 75 watts of laser power with the cone-flow meter to be described next. The cone-disc power

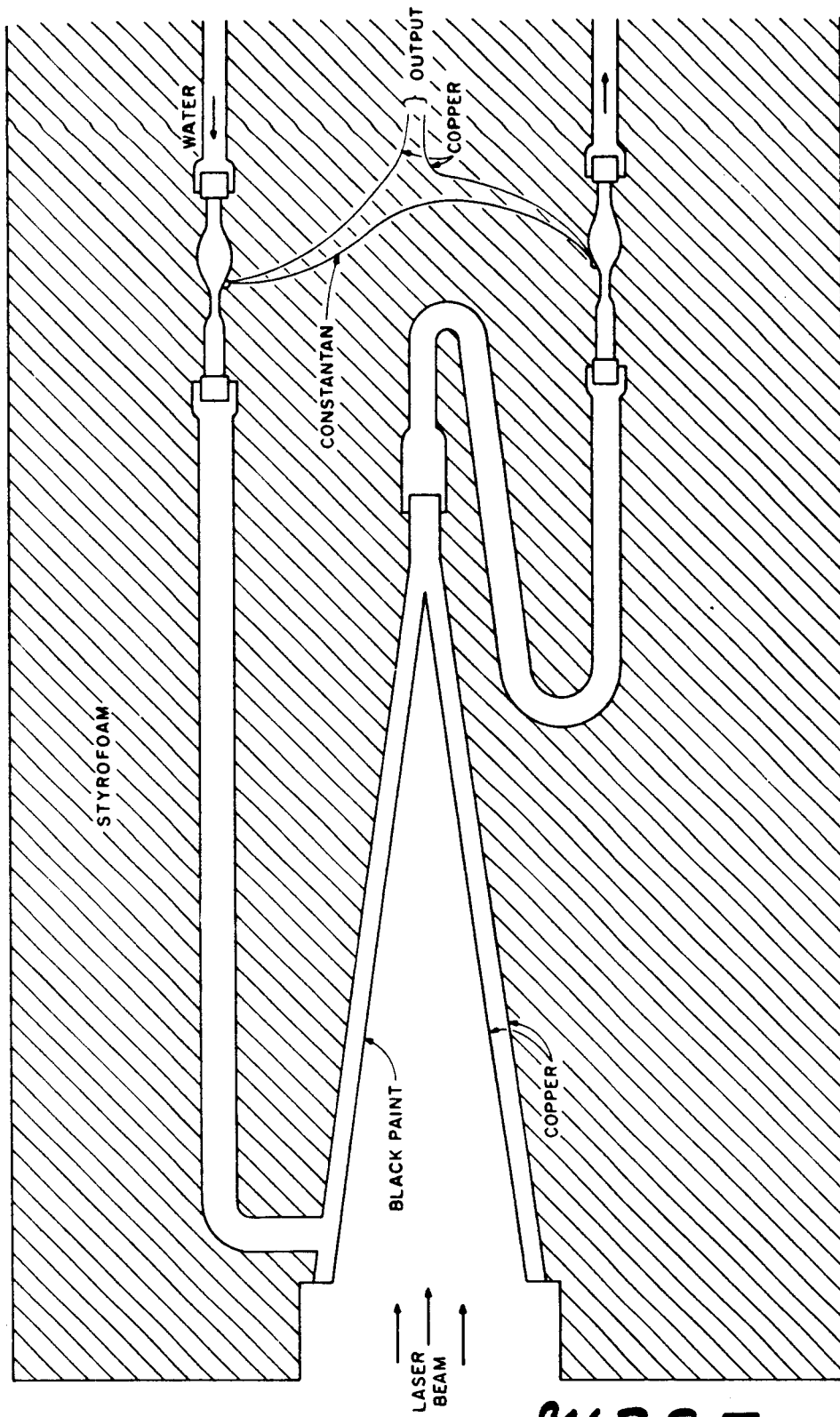


Figure 5-3. Schematic of the one-flow power meter showing construction details.

94397

meter was abandoned in favor of the cone-flow power meter, since the cone-flow power meter had none of the mentioned defects of the cone-disc meter.

### c. The Cone-Flow Power Meter

The cone-flow power meter shown in figure 5-3 has proved to be the most useful and accurate one which we have used thus far. The laser power is used to increase the temperature of water flowing through the double cone. The flowing water in contact with the inner, heat absorbing cone, maintains its temperature near room temperature so that radiation and convection are negligible. The reflection from the blackened cone was measured to be less than 0.2%. The water flow rate was maintained by a pressure regulator and metered with a calibrated differential flow meter. The flow rate was measured to an accuracy of 1%. The thermocouples were fastened on 3 cm pieces of 5.3 mm o. d., 4.6 mm i. d. copper tubing separated 10 to 12 cm, from the cone by tygon tubing. Electrically insulating epoxy held the junction on the tube, and a layer of conducting epoxy overcoated the entire junction to maintain its temperature

In order to assure a "mixed flow", the tube was crimped twice to an inner dimension of about 2mm; the two crimps were at right angles and were about 1 cm apart. The junction was located between the crimps. The cone and junctions were all isolated by an insulating plastic shield and an aluminum box. The usual water temperature was about 8°C and 75 watts of power produced a 1.25°C temperature rise with a flow rate of about 1 L/min. The overall response time was about 8 seconds with this flow rate. Since one could obtain the same accuracy with a 20°C temperature rise and could also quadruple the above flow-rate, one could easily measure 5 kilowatts with the same 3% accuracy.



A flow-cone of similar design has been used to measure 8.8 kilowatts<sup>1</sup>. Cones were constructed from both black dyed anodized aluminum and black painted copper. With the copper cone, the recorded thermocouple voltage had fluctuations of about 1% while with the aluminum cone the fluctuations were nearly 5%. Therefore, the copper cone was adopted for this power meter.

To check the accuracy of this power meter a teflon insulated resistance wire was wound outside a 1 mm thick copper cone about 6 cm long which was inserted snugly into the calorimeter cone. In this way the electrical power could be compared with the power measured by the calorimeter. Agreement within 2% was achieved; this agreement confirms our independent accuracy estimation of 3%. Thus, it is felt that the power meter is a reasonable choice for measurement from 1 watt to 5 kilowatts of CW laser power with accuracies of about 3%.

#### References

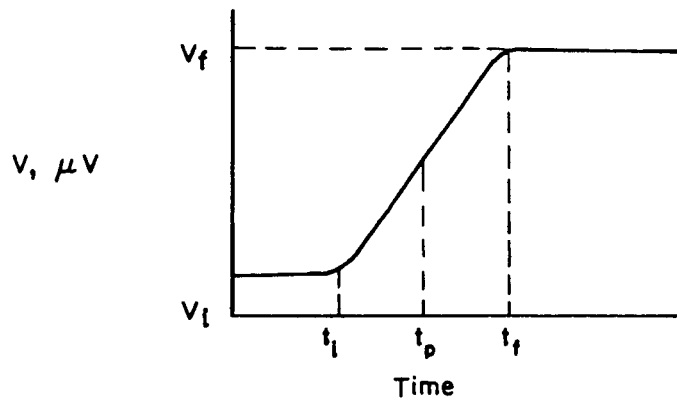
1. Technical Report. High Power Gas Laser Research. Raytheon Research Division, September 1968. Prepared for U. S. Army Missile Command, Redstone Arsenal, Huntsville, Alabama.

## 6. Data Reduction for the Liquid Cell Calorimeter

The measurement of the amount of energy in a laser pulse or the average power in a CW laser beam would be a simple matter if an ideal calorimeter could be employed. The calorimeter would consist of a cell which would convert all of the incident electromagnetic energy to heat energy. The heat energy in turn would raise the temperature of the cell from a temperature that represented the initial thermodynamic equilibrium state  $T_i$  to a higher temperature  $T_f$  which represents a final equilibrium state. If  $C$  represents the known heat capacity of the cell, the amount of electromagnetic energy incident could be determined from

$$Q = C (T_f - T_i) . \quad (1)$$

In this case the response time of the cell as well as the time duration of the input energy is immaterial since no energy is lost. Only the temperatures of the initial and final equilibrium states are relevant. A temperature time-curve would be as shown:



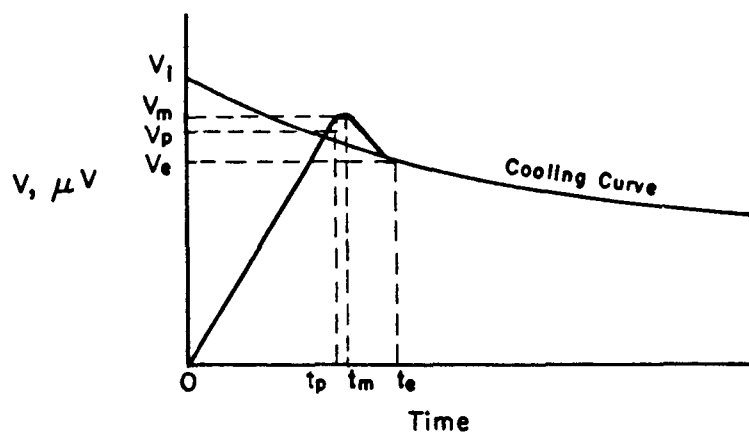
Where  $v$  is the temperature measured with a thermocouple and  $t_i$ ,  $t_p$  and  $t_f$  are times for the onset of the incident energy, the time the incident energy is turned off and the time the final equilibrium state is reached, respectively.

A real calorimeter inherently possesses two problems which prevent a simple determination of the injected energy as done above. Heat loss mechanisms exist during the time of and after the injection of the energy and the cell never reaches exactly a uniform temperature after the energy injection. However, for the calorimeter used here tests show that all of the electromagnetic energy entering the liquid cell is absorbed and that the absorbing properties of the liquid do not change with time for the energy levels and power levels used. In principle, it should be possible to set up the heat flow problem for the absorbing cell, from which the temperature distribution as a function of time and position could be determined and consequently predict the heat losses. The assumptions made in order to fit boundary conditions and to compensate for the complexities in the geometry of the absorbing cell make it difficult, if not impossible, to determine the heat losses to within the desired accuracy. Another alternative approach is to develop a technique of calibrating the calorimeter in such a way that when it is used to measure electromagnetic energy, the results can be stated with a confident accuracy.

The basic method of calorimeter calibration adopted here is to inject a known amount of joule heat energy into the calorimeter cell and measure the temperature rise with a calibrated thermocouple. Thus determining a calorimeter calibration constant in the units of microvolts (temperature rise) per joule (heat energy input). However, the calorimeter cell never reaches a uniform temperature and hence the problem

is to develop a technique of determining an effective temperature rise of the cell that will give an accurate calibration constant. Once the technique has been developed it can be applied to the measurement of electromagnetic energy.

The technique of measuring the temperature rise of the calorimeter cell is a result of an understanding of the calorimeter behavior under conditions of both measuring electromagnetic energy and that of calibration. Consider e. g. a typical temperature-time curve of the calorimeter cell under calibration condition:



An accurately measured amount of joule heat is injected into the calorimeter for a time  $t_p$ . The measured temperature rises almost linearly to  $v_p$  after which a slight overshoot with a maximum  $v_m$  at  $t_m$  takes place. Then the temperature decreases to  $v_e$  at a time  $t_e$  and beyond this point the temperature decreases at an exponential rate as a result of the heat loss mechanisms. It has been determined without exception and regardless of the source of heat, that the temperature decrease after the time  $t_e$  fits a simple exponential within the accuracy of measurement. With the aid of the temperature-time curve and a knowledge of the heat capacities and heat conductivities of the components of the

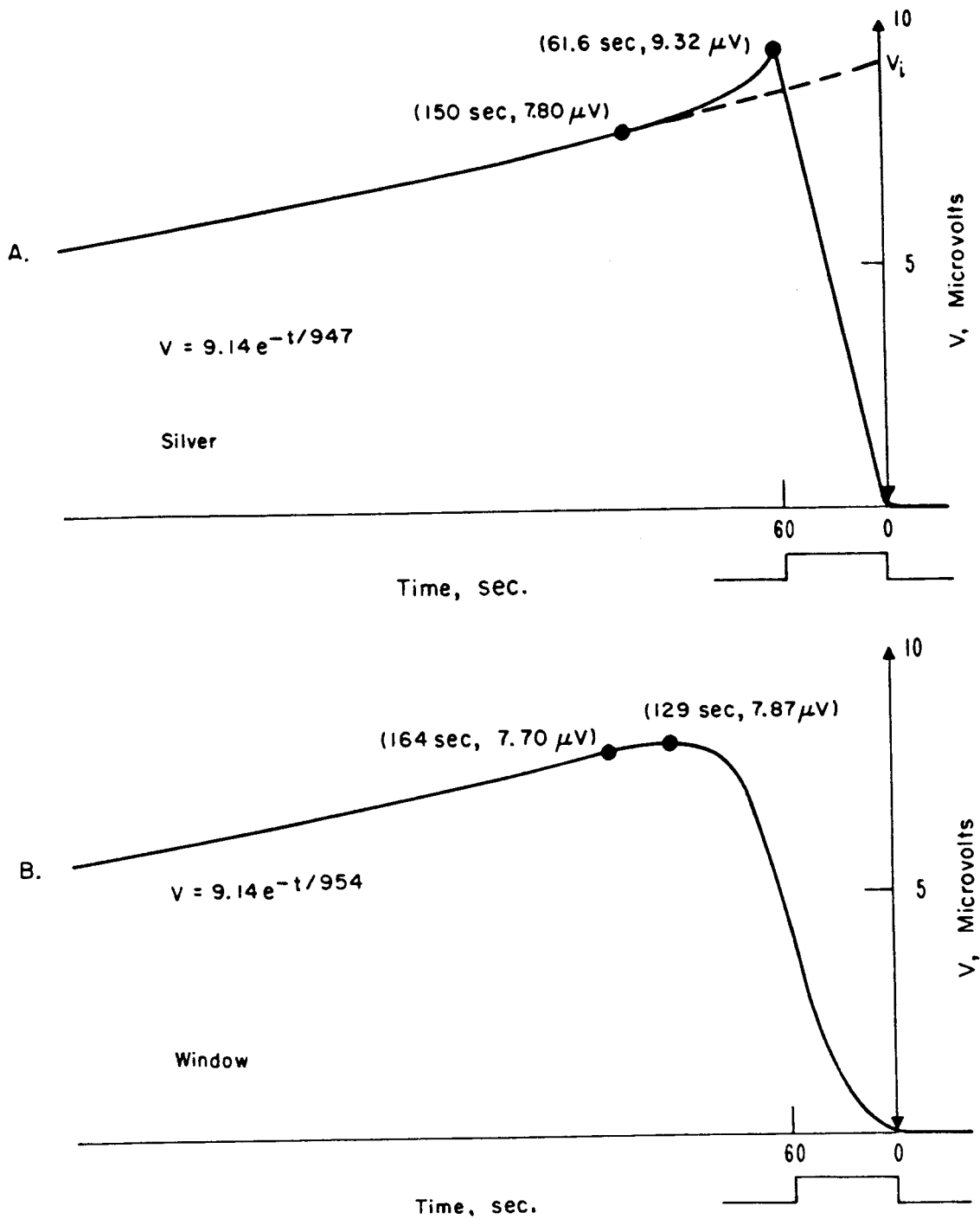


Figure 6-1. Response of calorimeter to a DC electrical energy pulse. Top trace shows the response of the silver surface and bottom trace shows the response of the quartz window.

calorimeter cell (quartz window, liquid absorbing medium and silver container), much can be inferred about the dynamics of the cell.

The temperature-time curve is a measure of the temperature of the silver container and this temperature is uniform over the silver surface compared to the rest of the cell. With the onset of the injected heat, the temperature of the silver rises directly as the heat is added until  $v_p$  is reached. Here, as a result of the relative heat capacities and heat conductivities of the three main elements of the cell, temperature gradients exist between the silver container and the absorbing liquid and the window (the former being the hottest). Between  $t_p$  and  $t_e$ , heat flows from the silver container into the liquid and the window to alleviate these temperature gradients until the point  $(t_e, v_e)$  is reached where the cell reaches a semi-isothermal state. For times after  $t_e$ , the loss mechanism is the predominant influence. Since the time constant of the heat losses is large compared to the response time of the cell, the gradients that exist within the cell are very small.

There are only two surfaces of the absorbing cell from which heat can be lost to its surroundings; the front surface of the window and the outside surface of the silver container. From the fact that a simple exponential function will fit the temperature-time curve, the predominant heat loss mechanism from the silver surface must be that which follows Newtons law of cooling and the heat loss correction can be evaluated on this basis. Figure 6-1 is a representation of the temperature-time curves of the center of the window and the silver container recorded simultaneously. Duration of the DC electrical input energy pulse was sixty seconds. The data from these curves are given in table 6-1.

Table 6-1. Data for Electrical Input

Energy	2.733 Joules
Pulse Duration	60 seconds
$(v_e, t_e)$ glass	(7.70 $\mu$ V, 164 sec.)
$(v_e, t_e)$ silver	(7.79 $\mu$ V, 150 sec.)
$(v_m, t_m)$ glass	(7.87 $\mu$ V, 129 sec.)
$(v_m, t_m)$ silver	(9.326 $\mu$ V, 62 sec.)

These curves show that the heat flows as described above during the heating period. Also, it can be seen that the window and the silver reach the same temperature at  $t_e$  and remain at the same relative temperature during the cooling period ( $t \geq t_e$ ) and hence to semi-isothermal condition. The difference between  $t_e$  for the glass and the silver can be explained by the difference in the response of the respective thermocouples as a result of difference in physical contact.

Establishing a procedure to determine an accurate calorimeter calibration constant essentially involves a procedure for determining a meaningful temperature rise of the calorimeter cell with which the known injected energy can be associated. The accuracy of the technique can be determined by comparing the electrically measured calorimeter calibration constant with one which is obtained from the known heat capacity (sum of the heat capacities of the components) of the calorimeter cell and the calibration of the thermocouple. The latter constant being that value which would be obtained from the results of calibrating a lossless calorimeter using eq (1).

A technique of fitting the cooling curve with an exponential and projecting the resulting equation back to zero time to obtain meaningful temperature rise,  $v_i$ , was first used. This procedure gives reliable results for calibration and laser energy measurements provided the ninety second dc electrical energy pulse length is used for calibration. In Section 6 the "reference time" is  $t = 0$ . However, it was later found that if the amount of injected heat energy was kept the same, but the time of injection was changed and of duration from fifteen seconds to three minutes, the value of  $v_i$  obtained from fitting the measured curves and hence the calibration constant,  $k_i$ , varied linearly with the duration of the injected energy pulse; with the lowest value determined for the shortest pulse. This phenomenon presents a problem when the same technique is used to determine the temperature rise of the cell while measuring power in a CW laser beam when the integration times are long compared to the cell response time.

The procedure that has been adopted is a result of two experimental facts (1) the cell does reach a nearly uniform temperature sometime after the injection of an electrical dc calibration pulse or energy injection from any other source and (2) the cooling curve is always that of a simple exponential.

Since the cell goes from an initial isothermal condition (before the onset of the injected energy) to a final nearly uniform temperature, a true temperature rise can be found if the temperature decrease due to the heat lost during the heating period ( $0 \leq t \leq t_e$ ) can be found.

During the cooling period ( $t > t_e$ ), the rate at which the temperature decreases as a result of the heat loss mechanisms is

$$\frac{dv}{dt} = -\frac{1}{\tau} v \quad (2)$$



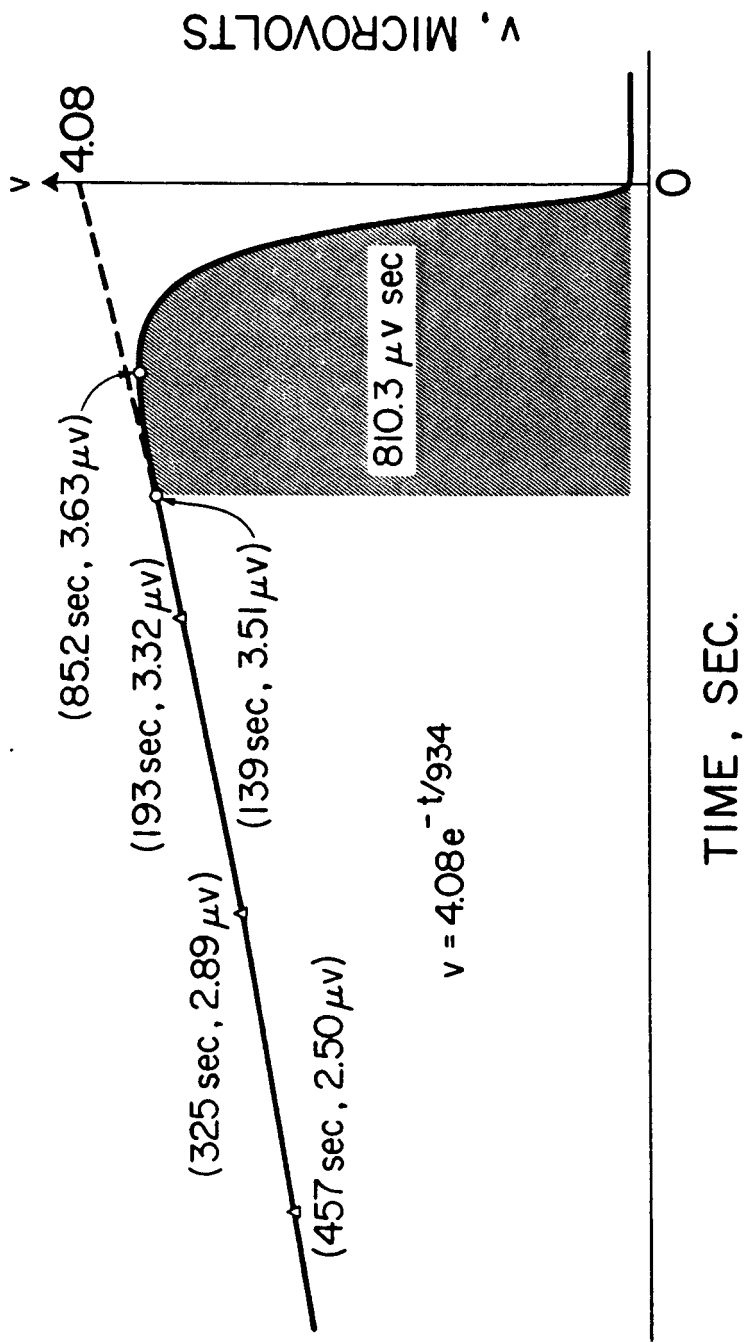


Figure 6-2. An example of the results of using the integration procedure in determining the amount of energy in a laser pulse. (See text).

Where  $v$  is the measured temperature difference between the cell and its surroundings and  $1/\tau$  is determined from the cooling curve. This indicates that the losses are a function only of the  $v$ . Then the decrease in temperature due to heat losses during the heating period should be

$$\Delta v = \frac{1}{\tau} \int_0^{t_e} v dt \quad (3)$$

the true temperature rise then would be the temperature  $v_e$  plus  $\Delta v$ . The quantity  $\Delta v$  can be found since  $v$  is measured during the heating period and  $\tau$  is known. The point  $(t_e, v_e)$  can be determined by comparing the function  $v_0 e^{t/\tau}$  with the measured curve.

The main problem is encountered when it is assumed that the temperature-time curve during the heating period as measured by the thermocouple attached to the silver container is the true temperature of the surfaces of the cell that can lose heat to their surroundings. It can be seen from figure 6-1 that during this time the temperature of the window center follows a similar curve, but it is not exactly the same and hence the error in this method.

When this procedure is used to determine the calibration constant from the injection of dc electrical energy, consistent results are obtained that are independent of the time duration of the injected energy and in addition that are consistently 3.5% below the thermocouple sensitivity divided by the heat capacity. The error may result from the departure from a uniform temperature condition in the cell during the heating period and the delay in the response of the thermocouple.

An example of the results of using the integration procedure in determining the amount of energy in a laser pulse are shown in figure 6-2, and given below.

$$v_e = 3.51 \mu v$$

$$\frac{1}{\tau} \int_0^{t_e} v dt = 0.43 \mu v$$

$$v_{\text{true}} = 3.94 \mu v$$

The calibration constant as determined by the same procedure is  $2.932 \mu v/\text{Joules}$ . Consequently, the energy contained in the laser pulse is 1.34 Joules. The energy measurement made by the plate described in Section 6 gives a value of 1.36 Joules. The agreement is  $\sim 1\%$ .

An example of the application of the integration method to the measurement of the average power in a CW laser beam is shown in figure 4-3. The experimental data from the curve are as follows:

$$v = (3.19 \mu v)e^{-t/1200} \quad t \geq t_e \quad \text{curve fitting}$$

$$\int_0^{t_e} v dt = 347.5 \mu v \text{ sec}$$

$$\tau = 1200 \text{ sec}$$

$$\Delta v = 0.29 \mu v$$

$$(t_e, v_e) = (211 \text{ sec}, 2.67 \mu v)$$

The approach here has been to rely on experimental data rather than theoretical analysis to suggest a technique for determining the energy seen by the calorimeter. Results thus far indicate that the integration procedure yields values for the calorimeter constant with

acceptable precision. Although the measured constants are lower than the heat capacity value by 3.5%, the error is always in the same direction. Since the same procedure is used for measuring the temperature rise during the laser power and energy measurements, the effect is a partial cancellation of the error. Consequently, the integration procedure possesses a high degree of precision and allows the measurement of laser power and energy with an accuracy of better than 2%.